7-19-2006

Electrical Characterization Of Metal-To-Insulator Transition In Iron Silicide Thin Films On Silicon Substrates

Hasitha C. Weerasinghe
University of South Florida

Electrical Characterization Of Metal-To-Insulator Transition In Iron Silicide Thin Films On Silicon Substrates

by

Hasitha C. Weerasinghe

A thesis submitted in partial fulfillment
of the requirements for the degree of
Master of Science
Department of Physics
College of Arts and Sciences
University of South Florida

Major Professor: Sarath Witanachchi, Ph.D.
Dale Johnson, Ph.D
Myung K. Kim, Ph.D.

Date of Approval:
July 19, 2006

Keywords: pulse laser deposition, hall voltage measurements, iron probe, iv characteristics

ACKNOWLEDGMENTS

I would like to thank my supervisor Dr. Sarath Witanachchi, for his suggestions and unwavering support. His vast experience and creativity helped me greatly along the way, and were essential to completion of this thesis. I would also like to thank Professor Dale Johnson and Professor Myung K. Kim for agreeing to serve as my faculty advisor, and providing advice when needed.

Further, my thanks goes to my lab-mates Boby Hyms, Malek Marik, Dr.Vaithianathan Veeramuththu and Gayan Dedigamuwa for their help they have given me and the long mind opening discussions.

And last, but not least, thanks to my parents, sister Pabasara and brother Uditha who encouraged me along and helped me though, the difficult times.

TABLE OF CONTENTS

LIST OF FIGURES AND TABLES

Electrical Characterization of Metal-to-Insulator Transition in Iron Silicide thin films on Silicon substrates

Hasitha C. Weerasinghe

ABSTRACT

Iron Silicide (FeSi) films deposited on silicon substrates with the native SiO_2 layer have shown a Metal-to-Insulator Transition (MIT) of more than four order of magnitude change in resistance. Modification of the SiO_2/Si interface due to Fe diffusion has been attributed to the formation of this effect. In this research a systematic experimental investigation has been carried out to study the effect of the growth parameters and substrate doping type in the transition. In addition, transport properties of continuous and discontinuous films have been investigated to understand the mechanism of this metal-to-insulator transition.

Four probe measurements of films deposited in *p*- and *n*-type doped Si substrates with resistivity in the range of 1-10 Ωcm showed similar temperature dependent resistance behavior with transition onsets at 250 K and 300 K respectively. These results indicate that the current transport takes place via tunneling through the SiO_2 layer into the Si substrate up to the transition temperature. Current appears to switch to the film after the transition point due to the development of high interface resistance. Discontinuous

FeSi films on silicon substrates showed similar resistance behavior ruling out possibility of current transport through inversion layer at the SiO_2/Si interface.

To investigate the role of the magnetic ion Fe, transport measurements of FeSi films were compared with those of non-magnetic metals such as Platinum (Pt) and Aluminum (Al). Absence of Metal-to-insulator transition on Pt and Al films show that the presence of magnetic moment is required for this transition.

Temperature dependent Hall voltage measurements were carried out to identify the carrier type through the substrate for FeSi films deposited on *p*- and *n*-type Si substrates. Results of Hall voltage measurements proved that the type of conductivity flips from majority carriers to minority after the transition.

Metal-to-insulating transition behavior of FeSi films depending on different laser fluences has been also investigated. Our results revealed as laser fluence is increased observed transition of the FeSi films reduces rapidly showing a highest magnitude of transition of about 1 MΩ for the films deposited with lowest laser fluence (0.64 J/cm^2) and a lowest of about 10 Ω for the films deposited with highest laser fluence (3.83 J/cm^2). Ion probe measurements indicated that the average kinetic energy of the ablated ion in the plume is considerably increased with the increase of the laser fluence. Consequently, magnitude drop in the transition can be considered due to the deeper penetration on Fe ion through the SiO_2 layer.

Thickness dependence study carried out for FeSi films deposited with high and low laser fluencies indicated transition slightly drops as thickness is increased, concluding the current transportation through the film becomes dominant after the transition temperature.

Chapter 1

Introduction

Metal-insulator-semiconductor (MIS) elements are widely used in modern electronics technologies such as field effect transistors, [H. H. Wieder(1978), [D.K.Ferry(1984), D.L.Lile, et al (1984)], chemical sensors [I.Lundstrom et al (1989)], and in solar cells [G.Rajeswaran et al (1983)]. Beside this direct involvement in technological products, the physics and Chemistry of MIS structures remains of fundamental scientific interests. For example, the knowledge of chemical and physical properties of a wide variety of metals in thin insulation layers on semiconductors is of importance in finding suitable metallization schemes, which is useful for the advancement of further technological process in the search for such stable contacts.

Metal-to-insulator transition (MIT) observed in different materials has been a great interest among the scientific community for several decades. MIT in variety of material systems observed, including Cr doped V_2O_3, [D.B. McWhan et all (1969)], VO_2, T_2O_3, VO_2 are shown in the Figure 1.1.1 [N. F. MOTT (1969)]. Intensive study of these systems have been conducted by Mott and Anderson and the onset of the transition had been attributed to charge carrier localization effects. Both the Anderson and the Mott transitions are variations of the metal-insulator transition. Mott transition takes place due to the electron-electron interaction whereas the theory of Anderson's transition is developed in a single electron picture.

Investigation of pulse laser deposited (PLD) FeSi films deposited on Si substrates at Laboratory for Advance Materials and Science and Technology (LAMSAT) has shown an anomalous metal-to insulator transition at much higher temperature than transition temperatures for other systems.[S.Withnachchi. et all (2006)]

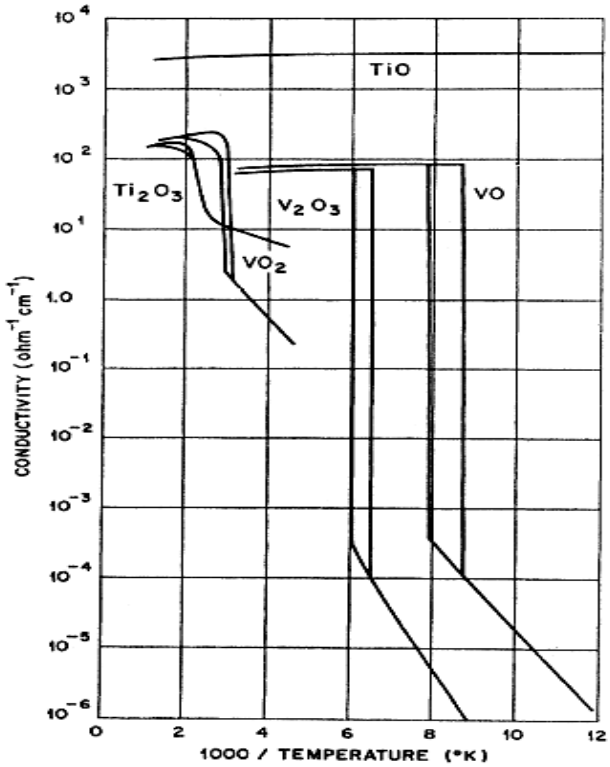

Figure 1.1.1 Metal-to-insulator transition observed in different metal oxide systems. [N. F. MOTT (1968)]

Temperature dependant resistance of FeSi film on a Si substrate is shown in Figure 1.1.2. (H. Abou Mourad PhD Thesis). A systematic investigation of FeSi films on Silicone substrates has shown that the interfaces between FeSi/ SiO_2 and SiO_2/Si are responsible for the transition. Transmission electron microscopy (TEM) studies have detected diffusion of Fe through native SiO_2 layer (~2nm thick) even for film deposited at room temperature. Unlike the well-established Mott like Metal-to –insulator transitions, which are characteristic of the material system, the observed MIT in FeSi/Si/Si system

results from the interaction between FeSi film and the Si substrate, across the Ultra-thin SiO_2 layer. In -plane conductivity measurements and Transmission Electron Microscopy (TEM) analysis of the FeSi/SiO_2/Si have also been conducted. Formation of multiple valance states of Fe in diffusion through the SiO_2 layer (discussed in the later part of this chapter), leading to charge carries hopping through insulating SiO_2 layer at high temperature, has been identify as mechanism of carrier transport from film to the Si substrate. Exponential increase of $(Fe^{+/++}B^{-})^{0/+}$ pairs formed due to coulomb interaction and localization of electrons, with the decrease of the temperature has been considered as the reason for the observed transition and this concept been well proved by incorporating experimental results with the three-layer mode[S.Withnachchi. et all (2006)]l.

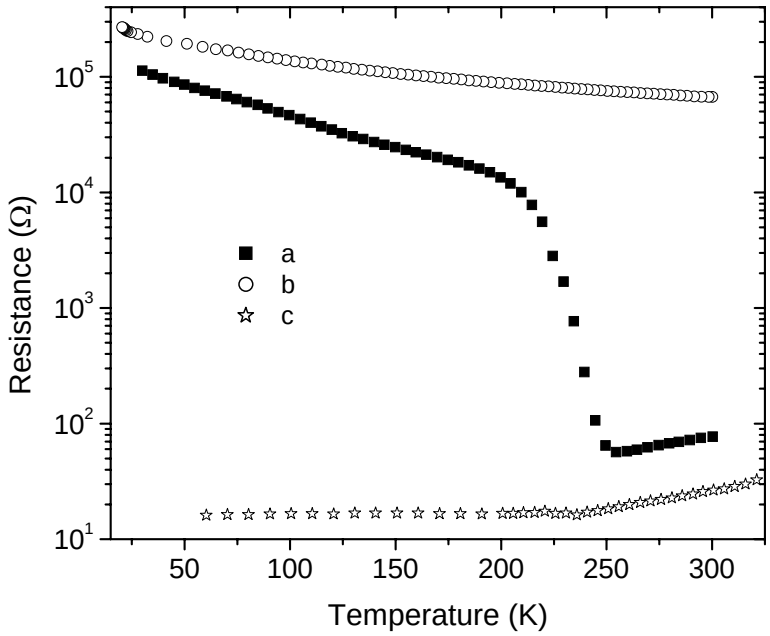

Figure 1.1.1 Temperature dependence of the resistance of FeSi films deposited at 400°C on (a) p-type silicon substrate of resistivity 1- 10 Ω-cm, (b) sapphire substrate. Curve (c) shows the temperature dependence of resistance for the etched silicon substrate. [S.Withnachchi. et all (2006)]

Dai et al have reported similar transition with low magnitude when Cupper (Cu) and Cobalt (Co) is deposited on p-type Si substrates by using vacuum sputtering at room temperature. [J.Dai et al (2000)]. This transition shows a similar shape and starts at the same temperature when compared with the transition discussed in the previously mentioned literature by Witanachchi et al. Dai et al attributed the observed transition to the conducting channel switching between the deposited upper metallic film and the silicon inversion layer observed in the TEM micrograph. Additionally temperature dependence of $Cu_{80}Co_{20}$ films deposited on SI substrates using PLD technique also exhibited a transition that started at 270 K.

We present in this thesis, results of set of experiments carried out to understand the mechanism of charge transport in the FeSi/ SiO_2/Si structures.

First efforts of the work presented in the dissertation were aimed at studying the effect of substrate doping type (*p*- and *n*-type) on the transition. Secondly, transport properties of discontinuous FeSi films on Si substrate were studies to investigate the possibility of current transport through an inversion layer at the SiO_2/Si interface as described by Dai et all. WE have also isolated a single FeSi/ SiO_2/Si junction to study the IV characteristics for both forward and reverse bias conditions. In addition, temperature dependant Hall measurements were performed to study the behavior of the carrier before and after the transition. We have used these results to identify a possible mechanism for the observed Metal-to-insulator transition.

Thirdly, formation of an Ohmic contact to a Si through the native SiO_2 layer at room temperature was studied by comparing the transport properties of Pt/ SiO_2/Si and Al/ SiO_2/Si with those of Pt/FeSi/ SiO_2/Si and Al/FeSi/SiO2/Si structures.

It has been shown that the substrate temperature during the growth alters the transition characteristics. This has been attributed to enhanced Fe diffusion. [S.withnachchi. et all (2006)]. We have studied the effect of the laser fluence on the transition, where high fluence is expected to increase the kinetic energy of the depositing special that would lead to enhance diffusion.

Chapter 2

Literature Review

2.1 Iron Silicide

Iron Silicide (FeSi) is a fascinating material that has been studied already many years ago for its unusual magnetic and thermal properties [Jaccarino et al (1967)]. Nowadays this system is object of renewed interest. In fact during the last five years many theoretical and experimental investigations of the magnetic and electronic properties have been reported. At low temperature FeSi shows an insulating behavior characterized by a nonmagnetic ground state whereas at room temperature it behaves as a paramagnetic 'dirty' metal.

The magnetic susceptibility exhibits a broad maximum at approximately 500 K and for higher temperatures that describes Curie-Weiss law [Jaccarino et al (1967)]. On the other hand, upon reducing the temperature below 500 K, the susceptibility drops nearly exponentially and vanishes below 50 K.[Jaccarino et al (1967)]. The temperature dependence of the resistivity is elaborated in the Figure 2.1.1. this material presents a gradual change in its resistivity bellow 300K, changing its transport properties from a dirty metal to a semiconductor. The change in the resistivity is gradual and covers a broad range of temperature as seen in the Figure 2.1.1.

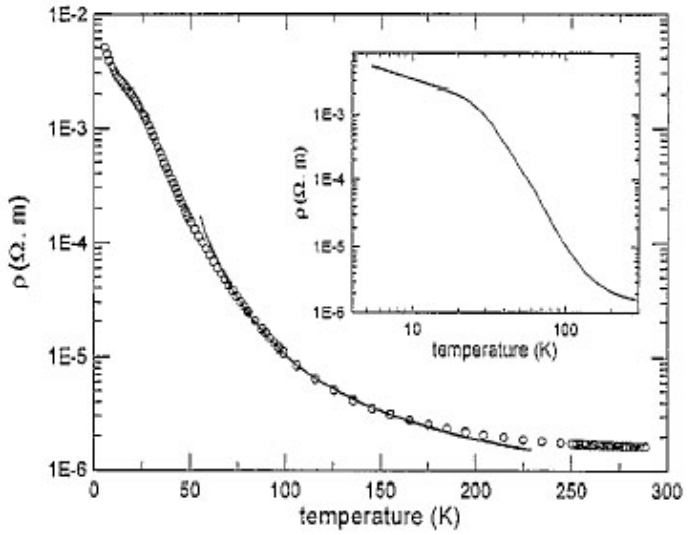

Figure 2.1.1 Resistivity dependence on temperature of FeSi bulk material. [Mihalik et al., J. Magt. Magt. Mater, 1996].

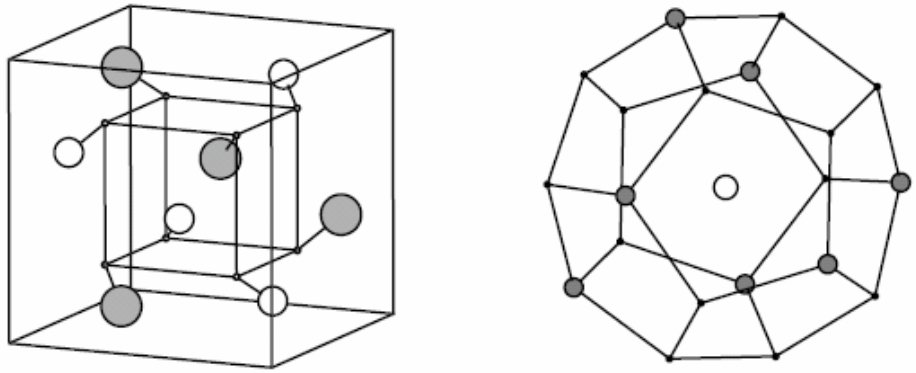

(a) (b)

Figure 2.1.2 (a) The unit cell of the cubic B20 crystal structure of FeSi. Shaded circles: Si atoms; open circles: Fe atoms. The atoms are connected to their positions in the B1 phase by solid straight lines. The four atoms of each type are at (u, u, u), (0.5 + u, 0.5 − u,−u), (−u, 0.5 + u, 0.5 − u) and (0.5 − u,−u, 0.5 + u), with different values of u for Fe and Si (b) The regular pentagonal dodecahedron surrounding an Fe atom in the 'ideal' B20 phase, showing the seven Si nearest neighbors. [A.Ial-sharid et al (2001)]

The atomic arrangement of cubic compound FeSi, with B20 crystal structure is schematically shown in the figure 2.1.2 a and 2.1.2 b . The B20 phase has space group P213, with eight atoms per unit cell. The B20 structure can be fully determined by three structural parameters: the lattice parameter, *a*, and two internal parameters, *u* and *v*, which determine the Fe and Si atomic positions in the unit cell, respectively. Another important feature to note is that each of the Fe and Si atoms in the 'ideal' B20 structure has seven nearest neighbors of the other type. The neighboring atoms lie in seven out of the 20 vertices of a regular pentagonal dodecahedron as shown in figure 2.1.2b. For this B20 structure, $u = -v = 1/4\tau = 0.154\ 51$

V.I.Kaidanov et al (1968)] V.I. Kaisdanov et. al. have examined the magnetic and electrical properties of FeSi, and concluded that nano-sillicide material properties are governed by their 'd' electrons, which do not participate in bonding. More recently, J F DiTusa et al (1996), G.Aeppli et an (1999)] demonstrated FeSi as a 'Kondo insulator'.

The study on electronic properties of FeSi using local-density-approximation (LDA) by means of linear augmented-plane-wave (LAPW) band calculations has shown the evidence that FeSi is a small band-gap (0.5-0.11 eV) semiconductor containing sharp density of state (DOS) features nearby Fermi energy (E_F) [L.F. Matthesis and D.R. Hamann, (1993)]. In order to study the changes in the band-gap and in the density of states as a function of temperature, A.Chainani et al. [A Chainani et al (1994)] have employed high-resolution photoemission spectroscopy. Consequently, they have observed an extremely small band-gap in the density of states of FeSi in the semiconducting phase.

Surface analysis of Fe films grown on SiO_2 /Si substrates, done by Ruhrnschopf et al. [K.Ruhrnschopf et al (1997)] revealed the evidence for Fe diffusion through the SiO_2 layer even at the room temperature growth. In this study, FeSi was formed after being annealed at 600 ^oC, Indicating that complete diffusion of Fe film into Si, thus forming FeSi . In addition, several other studies have also been performed on FeSi and $FeSi_2$ film growth directly on Si substrates. [N. G. Galkin et al (2001), Z. Liu, et al (1998)]

Anomalous metal-to-insulator transition in FeSi films deposited on SiO_2 /Si substrates has been first observed by Witanachchi et. al. [S. Witanachchi, H. Abou Mourad, and P. Mukherjee (2006)], in which, they claimed that the transition was due to the diffusion of Fe ions through the SiO_2 layer. Also, they proposed a three-layer model explaining the transition and investigated the transition behavior depending on the substrate temperature.

2.2 Silicon Dioxide

Under exposure to oxygen, the surface of the Si wafers oxidizes to form silicon dioxide (SiO_2). This native SiO_2 of a typical thickness of 10-20 A^o, is a high-quality electrical insulator and can be used as a barrier material during impurity implants or diffusion. SiO_2 layer plays a major role in semiconductor devices such as metal oxide semiconductor (MOS) transistors, multilevel metallization structures such as multichip modules. The ability to form a native oxide was one of the primary processing considerations, which led to silicon becoming the dominant semiconductor material used in integrated circuits today.

Chemical reactions of the oxidation occur on the surface of the substrate in the presence of pure oxygen or water vapor conditions can be given as:

$$Si + O_2 \longrightarrow SiO_2$$

$$Si + 2H_2O \longrightarrow SiO_2 + H_2$$

First reaction is usually known as “Dry oxidation” whereas the second, which occurs in the presence of moisture is known as "Wet oxidation”. Oxygen arriving at the silicon surface can then combine with silicon to form SiO_2.

Initially, the growth of SiO_2 is a surface reaction only. However, after the SiO_2 thickness begins to grow, the arriving oxygen molecules must diffuse through the growing SiO_2 layer to get into the silicon surface in order to react. The Si/SiO_2 interface has number of unique electronic and structural properties of enormous importance to electric properties and has been extensively studied by several research groups. Transmission electron microscopy (TEM) and x-ray scattering studies have indicated that presence of the oxide layer [O.L. Krivanek et al (1978), P. H. Fuoss and L. J. Norton (1988)] in Si substrate. It has been found that the SiO_2 layer plays a major role in the metal-to-insulator observed in $FeSi/SiO_2/Si$ structures.[S. Withnachchi. et all (2006)].

Chapter 3

Preparation of FeSi thin films by pulsed laser deposition (PLD)

3.1 Pulsed laser Deposition

FeSi thin films studied in this dissertation were grown by pulsed laser deposition (PLD) technique. Laser ablation has gained a great deal of attention in the past few years for its ease of use and success in depositing materials of complex stoichiometry. PLD was the first technique used to successfully deposit a superconducting $YBa_2Cu_3O_7$-d thin film. Since then, many materials that are normally difficult to deposit by other methods, especially multi-element oxides, have been successfully grown by PLD. The main advantage of PLD derives from the laser material removal mechanism; PLD relies on a photon interaction to create an ejected plume of material from any target. The vapor (plume) is collected on a substrate placed a short distance from the target. Though the actual physical processes of material removal are quite complex, one can consider the ejection of material to occur due to rapid explosion in a small area of the target surface due to superheating. Unlike thermal evaporation, which produces a vapor composition dependent on the vapor pressures of elements in the target material, the laser ablation produces a plume of material with stoichiometry similar to the target. It is generally easier to obtain the desired film stoichiometry for multi-element materials using PLD than with other deposition technologies. Moreover, energy of the ablated species take a vast range from about 2eV to 30 eV.

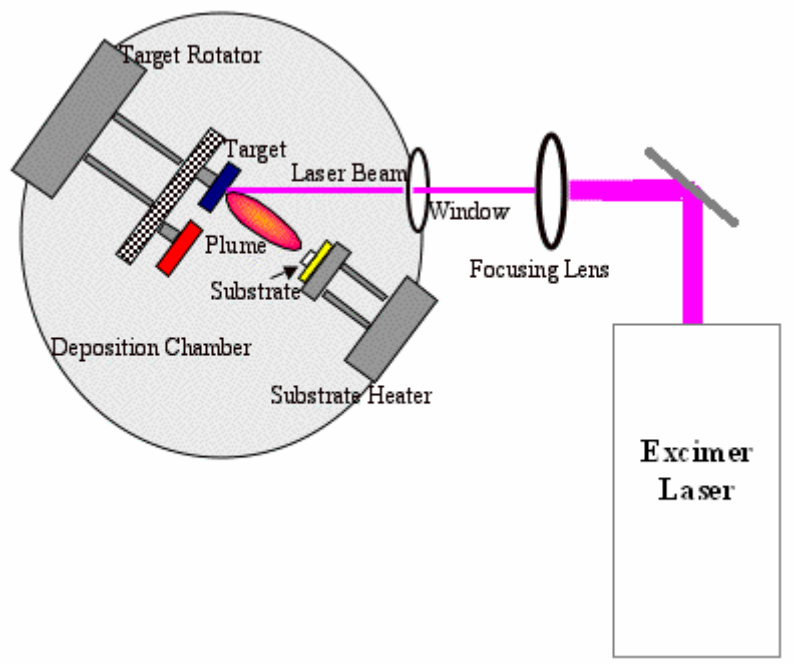

Figure 3.1.1 The PLD system used to deposit the Iron Silicide films.

The layout of a PLD system is simple and depicted in figure 3.1.1. It consists of an excimer laser acting as the power source, a deposition chamber that contains both target and the substrate, and optics (mirrors and a lens) that are, respectively, used to direct and focus the laser beam on the target. The book written by G. K. Hubler (1994) can be referred as an excellent review of PLD.

When the laser radiation is absorbed by a solid surface, electromagnetic energy is converted first into electrical excitation and then into thermal, chemical, and even mechanical energy to cause evaporation, ablation, excitation, plasma formation, and

exfoliation. evaporants form a “plume” consisting of a mixture of energetic species including atoms, molecules, electrons, ions, clusters, micron-sized solid particulates and molten globules.

This process attributes to many advantages as well as disadvantages. Advantages are flexibility, fast response, energetic evaporants and congruent evaporation. The disadvantages are presence of micron-sized particulates, and the narrow forward angular distribution .

3.2 Film growth:

3.2.1 Silicon Substrates

In this study silicon substrates with different orientations and resistivity have been employed for thin film deposition.

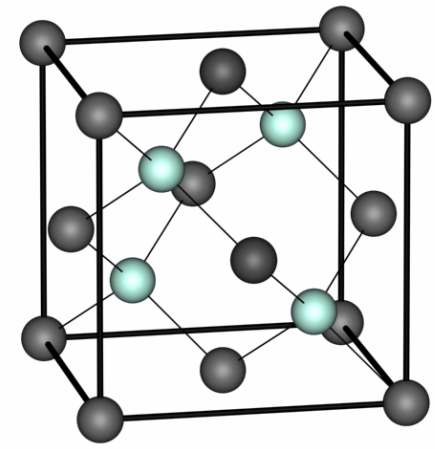

Figure 3.2.1 Silicon crystallographic structure. It has the diamond structure, which is two fcc structures shifted along the diagonal with respect to each other

Silicon crystallizes in the diamond structure with a lattice constant of 5.43 A^0. The diamond structure could be viewed as two face-center cubic Bravias lattice one side the

other but shifted along the diagonal by one fourth of its length as illustrated in the figure 3.2.1. It is known that Si is an indirect semiconductor, with a band gap value of about 1..12 eV when measured at 399K. [S. M. Sze (1985)]

In semiconductor production, doping refers to the process of intentionally introducing impurities into an extremely pure (also referred to as intrinsic) semiconductor in order to change its electrical properties. By doping pure silicon with group V elements such as phosphorus, extra valence electrons are added which become unbonded from individual atoms and allow the compound to be electrically conductive, n-type material. Doping with group III elements, such as boron, which are missing the fourth valence electron creates "broken bonds", or holes, in the silicon lattice that are free to move. This is electrically conductive, p-type material. In this context then, a group V element is said to behave as an electron donor, and a group III element as an acceptor.

The (100) oriented Boron-doped p-type Si, and Arsenic-doped n-type Si substrates with the resistivity varying between 1 and 10 Ω-cm were used for depositing FeSi thin films. Figure 3.2.2 shows the conductivity of Boron-doped p-type Si with a doping concentration of $10^{17}cm^{-3}$ as a function of temperature. As the temperature decreases from 400 to 120 K, the Boron-doped Si behaves like a degenerate semiconductor due to the high dopant concentration, where the resistivity (conductivity) exponentially drops (increases), however, it substantially increases (decreases) for further decrease in temperature (< 120 K) where it exhibits intrinsic semiconducting properties due to the alternation in to non-degenerate semiconductor with the decrease of the temperature. Note that the Boron-doped *p*-type Si substrate used in this study and the one used by Witanachchi et al in 2006, are the same. Also note that Figure is produced by

extracting data from a digitized figure containing the results of conductivity dependence on the temperature for silicon of different B dopant concentrations [F.J.Morin (1954)].

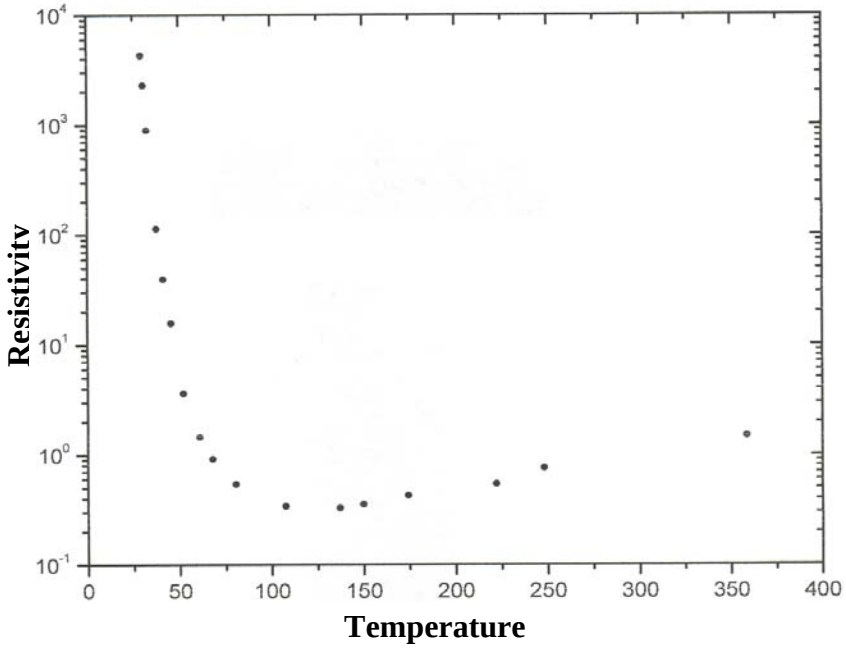

Figure 3.2.2: Resistivity depending on temperature for the Boron-doped p-type Si (Boron concentration in the sample is ~ 10^{15} atoms/cm^3).

3.3 Substrate cleaning and Deposition of FeSi films

Usually, chemical cleaning is used to remove surface contaminants of the substrates. Purpose of cleaning is to eliminate possible problems due to contamination or lattice imperfections at the interface. In study substrates were cleaned with acetone and methanol followed by deionized water in ultrasound baths. The substrates were first put in an acetone ultrasound bath for 10 minutes followed by 10 minutes in deionized water. Then it was moved to a methanol ultrasound bath for another 10 minutes. After the ultrasound baths were done the substrate was rinsed with deionized water and then blown dry with Nitrogen (Dry air).

After the substrate was cleaned it was mounted on a heating block facing the target, which would be used in the ablation process. Two methods were used in mounting the substrate to the heating block. Each method was implemented depending on the temperature at which the sample would be deposited. If the samples were to be deposited at room temperature, substrate would be mechanically pressed against the surface of the surface of the heating block by stainless steel tabs. If a high temperature deposition was to take place the substrate was mounted to the heating block by silver ink. This method ensures uniform heating of the substrate and eliminates any heat gradients that might present if the substrate was secured mechanically.

The commercially obtained FeSi target was 3.2 cm in diameter and 0.6 cm in thickness. It was fixed to a 1.2 cm Shaft connected to the target motor by means of a rotational feed through. The motor was used to rotate the target during the deposition to minimize the damage to the target from ablation process. The distance between the substrate and the target during deposition was set to 4 cm. Spot size of the laser beam in the target after focusing was measured by measuring the area of burn pattern of photographic paper after exposing it to ten pulses of laser placing the photographic paper on the target. This measurement was used to calculate the fluence, which is calculated by dividing the energy of the laser pulse by the area of the spot. The laser fluence at the target can be changed by moving the focusing lance. Pre-calculated fluence-lens position information was used to obtain the required laser fluence. Laser fluence of 0.6 to 4.0 J/cm^2 were used in the reported work.

Chapter 4

Sample Characterization

The samples were characterized using several techniques to gain information about the transport properties of the deposited films and their interaction with the underlining substrate.

The crystallinity of the films was studied using an x-ray diffraction (XRD) technique. D8/FOCUS x-ray diffraction system used for the x-ray diffraction of the FeSi target showed the characteristic x-ray peaks. However, films deposited at room temperature lack any peaks indicating the film to be amorphous.

The thickness of the samples was studied at the Engineering Metrology Laboratory by using EKTAK 30 30ST auto remote control stage profiler. A step was created by a mask during the film growth to enable the thickness measurements. The needle-like probe in the profilometer moves across the edge to record the film height. (Figure 4.1.1)

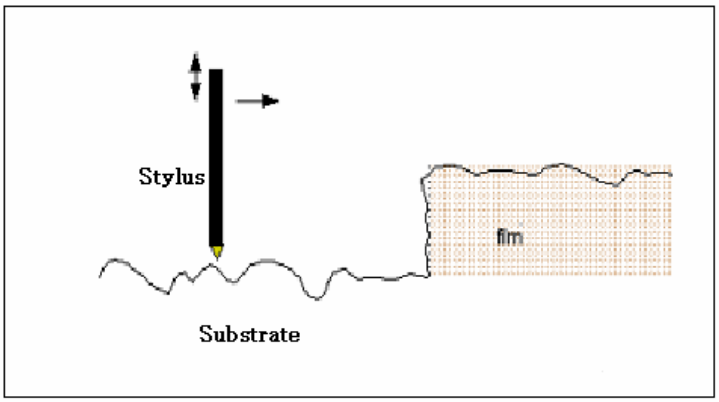

Figure 4.1.1: Principle of the Profilometer

4.1 Resistance and Current-voltage measurements

Transport properties such as Direct current (DC) resistance and Current Vs Voltage (IV) characteristics were investigated using a standard four-point probe method. After deposition was completed the sample was removed from the deposition chamber and 0.8cm x 0.3cm peace was cut off for testing. A 0.4mm piece of (0.25mm diameter) 99.998% Indium wire was cut and placed on the sample and then pressed carefully against the sample as shown in the figure 4.1.2 to form a good electrical contact. Four such contacts were made keeping the 0.2cm distance between each contact. The sample was then placed on a Cupper finger of closed-cycle refrigeration system (APD cryogenics HC-2). Silicon grease was used to fix the sample in place and also to have a better thermal contact with the cupper finger and the sample.

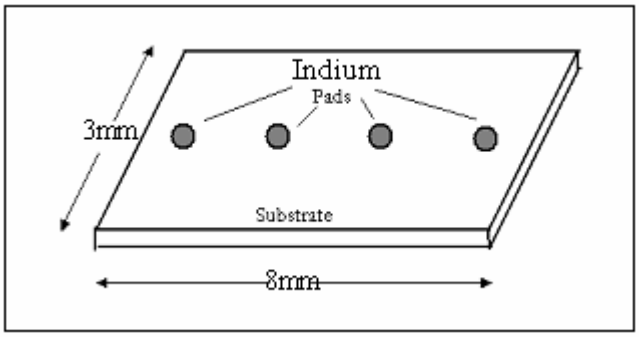

Figure 4.1.2: Schematic Diagram of the sample used for Resistance Vs. Temperature (RT) and current vs. voltage (IV) measurements

The copper leads were placed on the indium pads making sure that contacts have been made properly, by observing the reading on the voltage meter (voltage across the two inner leads) by passing 10 μA current through outer leads. This also conformed that the voltage applied to deliver the current was not exceeding the constant current power supply maximum voltage settings. Silver conducting ink was placed carefully on the

leads and indium contact pads to ensure that the leads would remain in electrical contact throughout the experiment. Sample was kept for about 2 hours until silver paint is dried and then tested for temperature dependant measurements.

A Schematic sketch of the system used for resistance measurements is illustrated in figure 4.1.2. The devices controlling the parameters of the measurement, (applied current, measured voltage and temperature control and reading) were controlled by a PC through a GPIB board. An APD cooling (HC-2) system and Lake Shore temperature controller were used to control the temperature. In combine, they maintained the temperature within a degree while measurements were being taken. A labVIEW program was used to control the temperature at which a measurement is to be taken, the temperature steps between measurements, the number of current pulse per measurement, and values of the current to be applied before a measurement is taken. Resistance was calculated using Ohm's law R=V/I, where V is the voltage measured across the inner leads of the sample and I is the applied current. This calculation was made when a current pulse was applied to the sample using Keithely 224 constant current source and the voltage measurement was done by a Keithely 182 nano-voltmeter. In order to obtain reliable results ten measurements were taken for every current value, five times in one current direction and other five current values in the opposite direction. An average and standard deviation of the voltage measured for every current value was taken and used to calculate an average resistance. The current pulses of 1ms duration was varied from 1 to 200 μA. Film Resistivity and the IV characteristics at different temperatures were obtained from the

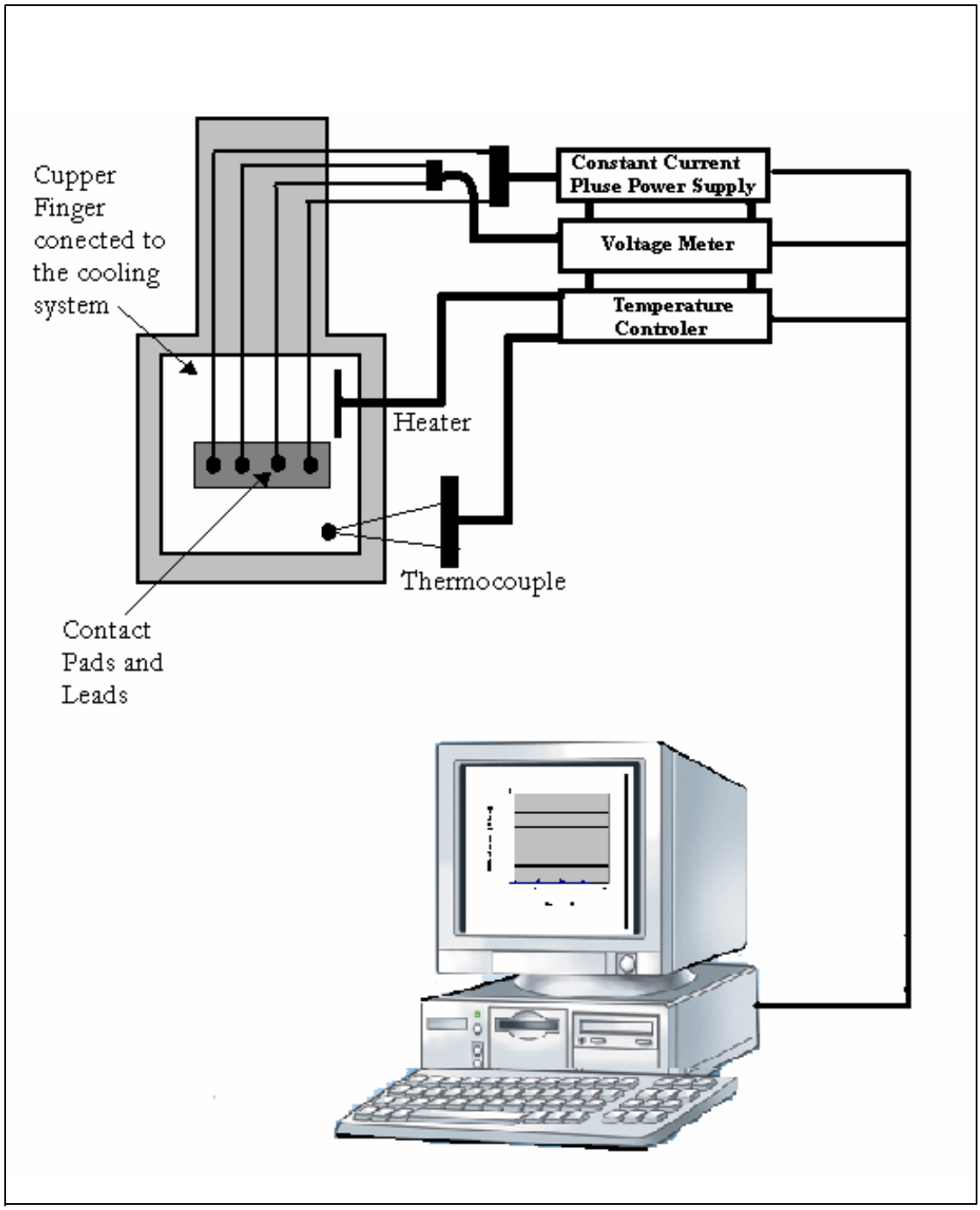

Figure 4.1.3 Schematic diagram of the temperature dependant resistance measurement system. A PC through a GPIB connection to the different devices controlled the measurement process, from applying the current pulse to measuring the voltage during the given temperature range.

same dataset. Finally these resistance calculations were plotted as function of temperature.

4.2 Hall Voltage measurements

Hall measurements are widly used in characterization of the semiconductors to measure carrier concentration and carrier mobility. Because of its simplicity, low cost, and fast turnaround time, it is an indispensable characterization technique in the semiconductor industry.

When a magnetic field is applied at right angles to current flow, an electric field E_H is generated which is mutually perpendiculer to the product of the current density and the megnetic induction.

Thus,

$$E_H = \frac{RBI}{A} \qquad \text{(A)}$$

$$V_H = \frac{RBI}{w} \qquad \text{(B)}$$

where ***R*** is the Hall coefficient. ***I*** the current through the sample, **A** the sample cross section, ***w*** the thisckness, and ***B*** the magnetic induction.

R as defined in Equation (A) and (B) is given by [Semiconductor Measurements and instrumentation By W.R Runyan]

$$R = \frac{-1}{nq} \text{ , } \frac{1}{pq} \qquad \text{(C)}$$

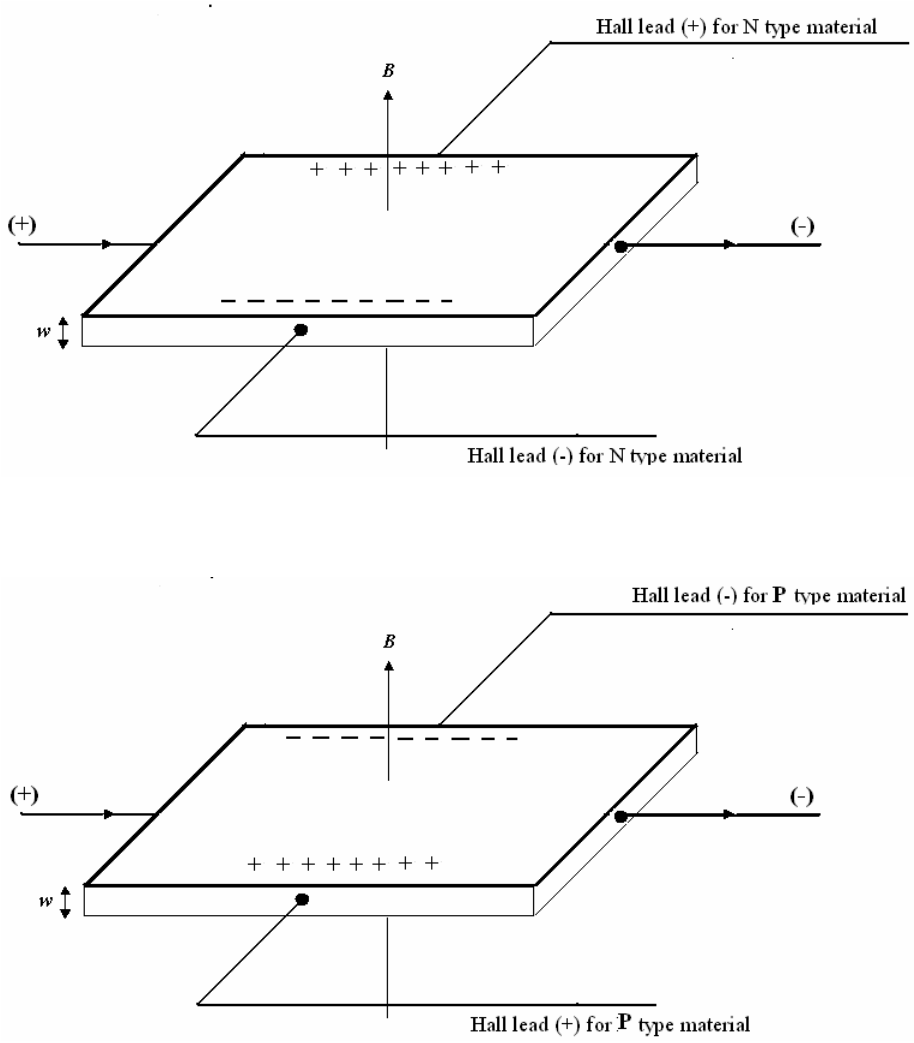

Figure 4.2.1 Basic principle used to identify the carrier type (sign convention)

where q is the electronic charge and n and p the density of carriers. Thus carrier type as well as concentration can also be determined from Hall valtage mesurements, since if the sing convention of figure 4.2.1 is followed, R is negative for n-type and positive for p-type.

Hence, when carrier type is unknown, one can identify the carrier type measuring the polarity of the Hall voltage.

Hall Voltage, V_H was calculated using formula given bellow.

$$V_H = \frac{V_1 + V_4 - V_2 - V_3}{4} \quad , \qquad \text{(D)}$$

where V_2,V_2,V_3 and V_4 are the Hall voltages measured for (+B,+I), (-B,+I), (+B,-I) and (-B,-I) respectively.

During the experiment Hall voltage was measured for both positive and negative current values for each temperature interval (starting from 320K down to 200K), applying a plus magnetic field and then similar procedure was followed for the negative magnetic field. Finally Hall voltage was calculated using equation (D) and plotted against the temperature.

Chapter 5

Transport Properties

Metal-to-insulator transition in laser-deposited FeSi films was first observed by Witanachchi et al. [Witanachchi et al. 2006]. Reproduced samples of FeSi were deposited on *p*-type Si substrates with the resistivity of 1-10 Ω-cm as outlined in Chater3. All the FeSi films presented in the report were prepared at room temperature with a laser fluence of 0.5 J/cm^2, while maintaining the chamber base pressure at 1×10^{-5} Torr. Transport properties of these films were investigated by two techniques. Films resistance was studies by the four-probe technique while the carrier type was determined by Hall measurements.

5.1 Temperature Dependence

Film resistance was measured in two different configurations. Four-probe measurements of continuous films provided information about the film-substrate interaction at different temperatures while isolated junction was probed by studying IV characteristics of discontinuous films.

a) Continuous FeSi films on Si substrates

The Figure 5.1.1 shows the dependence of resistance in FeSi specimens for different current values. It can be clearly seen from the figure that the films exhibit metallic behavior between the room temperature and 270 K, however, interestingly, resistance of the films sharply increases (transition) from about 100 Ω to more than 100

kΩ in the range of 260-230 K. For the temperature between 230 and 140 K, the change in the resistance is more gradual, followed by a degree in resistance below about 50K.

It is also clear from the figure that the onset of transition is relatively the same for all the applied current values. The lower the applied current values the higher the magnitude of transition, and *vice versa*.

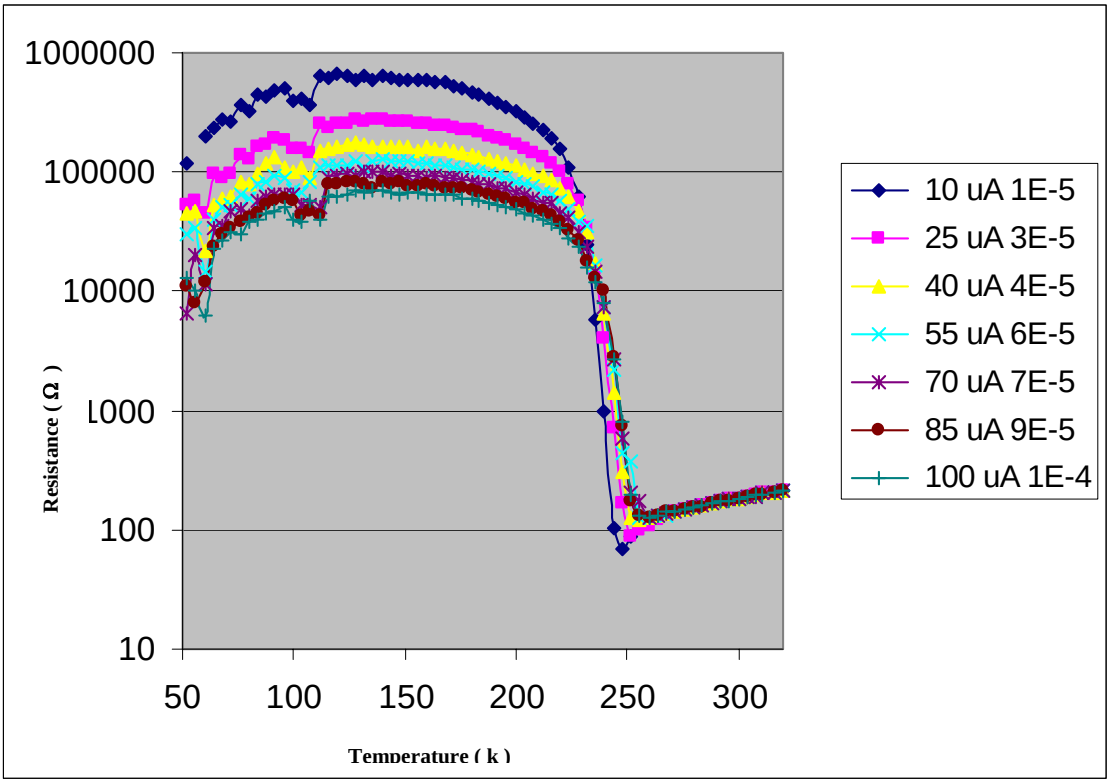

Figure 5.1.1 The resistance of FeSi films deposited on *p*-type Si depending on temperature for different applied current values.

The metallic behavior has been attributed by Witanachchi et. al, to the electron tunneling across the SiO_2 layer via impurity sites. Diffusion of Fe into SiO_2 leads to the formation of impurity bands with in the large band gap of the insulator.

Similarly FeSi films deposited on *n*-type 1-10 Ωcm silicon substrates were tested for temperature dependence on resistance. RT data displayed in the Figure 5.1.2, shows that the transition takes place at about 305 K, with similar shape and magnitude as observed for p-type substrates. Figure shows a metallic behavior with low resistance of about 7 Ω until the temperature decreased from 320 to 310 k. The resistance rapidly increased to about 20 kΩ in the temperature range of 310 to 257 K.

One of the interesting feature observed during the transition was, the significant dependence of resistance on the applied current near the transition. Figure 5.1.3 and Figure 5.1.4 are the detailed figure of the figure 5.1.1 and 5.1.2, which shows resistance dependence on the current during temperature range of 270 K and 220 K. Noting the line **AB** drown in the figure 5.1.3 at 250 K, it can be seen that the increase in current from 1 μA to 17.5 μA, has led to a increase in the resistance of two order of magnetite. This translates to a 06x10^6 Ω/A change, which is significant in high response devices.

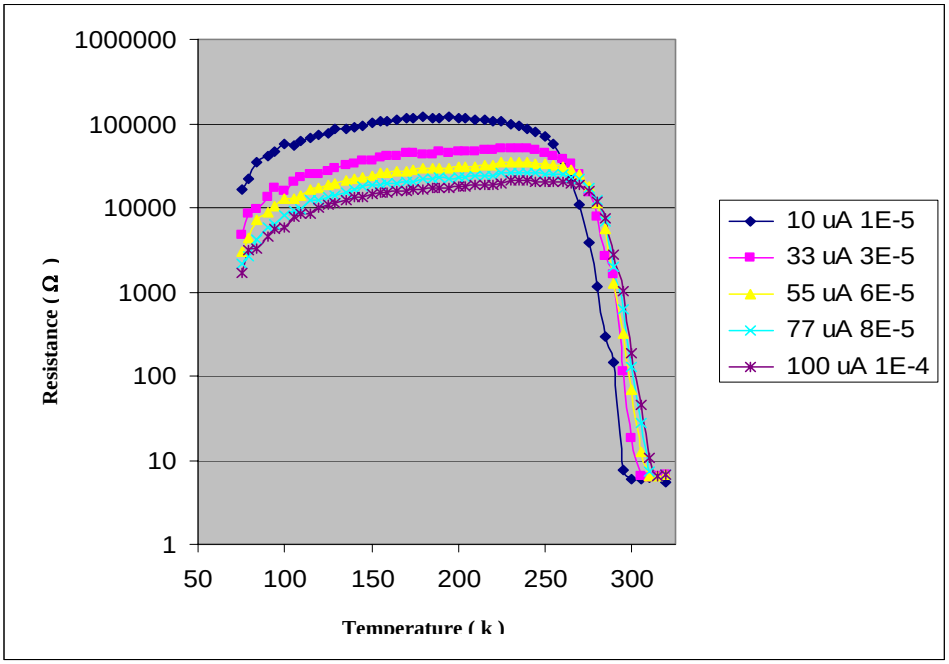

Figure 5.1.2 The temperature dependence of resistance of PLD-deposited FeSi films on n-type Si, for applied different current values

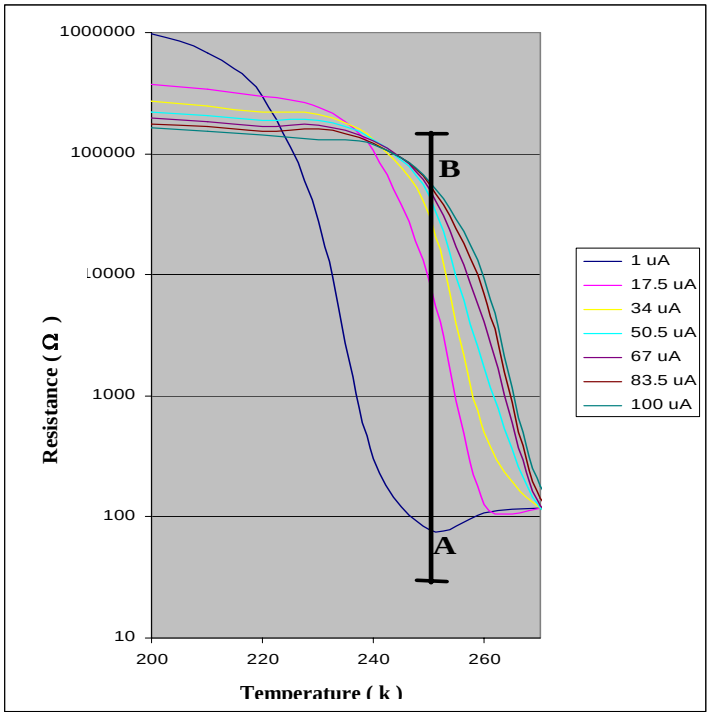

Figure 5.1.3 Current dependence of the resistance change for a film on a *p*-type substrate near the transition

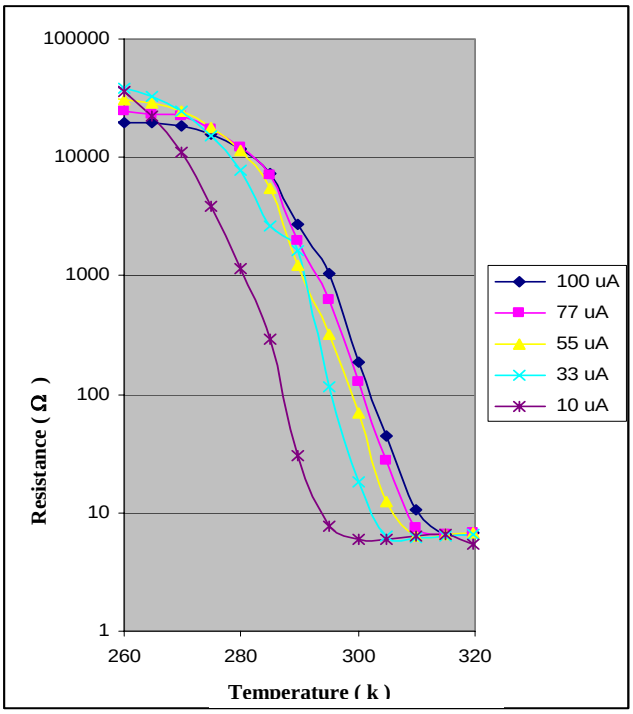

Figure 5.1.4 Current dependence of the resistance change for a film on a *n*-type substrate near the transition

Similar effect can be seen in the Figure 5.1.4 with a 7.6×10^7 Ω/A change during the transition.

It is easy to observe from above discussed data, a distinct transition in resistance with about four orders of magnitude takes place whenever FeSi is deposited on silicon substrates with 1-10Ωcm resistivity.

It is well known that interface states at the SiO_2/Si interface leads to the formation an inversion layer. The inversion layer of *p*-type substrate could have high electron density, and thus could be highly conductive. One of the possible explanations for the observed transition is that, electrons tunnel through the SiO_2 layer to the intersection and the current is transported with low resistance along the inversion layer. As the conductivity of the inversion layer is dropped with the decreasing temperature, the current is switched back to the film. To test validity of the argument we have conducted transport measurements on discontinuous FeSi films, where a continuous inversion layer at the SiO_2/Si interface states produced by Fe diffusion is not present.

b) Discontinuous FeSi films on Si substrates

Discontinuous FeSi films were deposited on *p*-type silicon substrate by placing a mask in the middle of the substrate during the film growth. The temperature dependant resistance measurements were taken by placing the current and voltage probes as shown in the Figure 5.1.5.

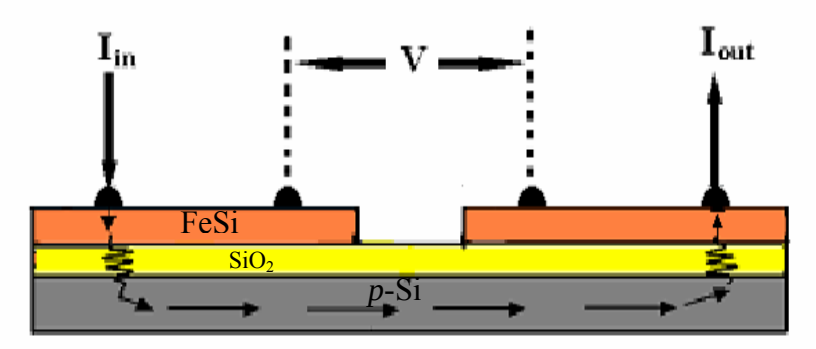

Figure 5.1.5 Schematic diagram of the voltage probe placement for isolated FeSi/Si interface

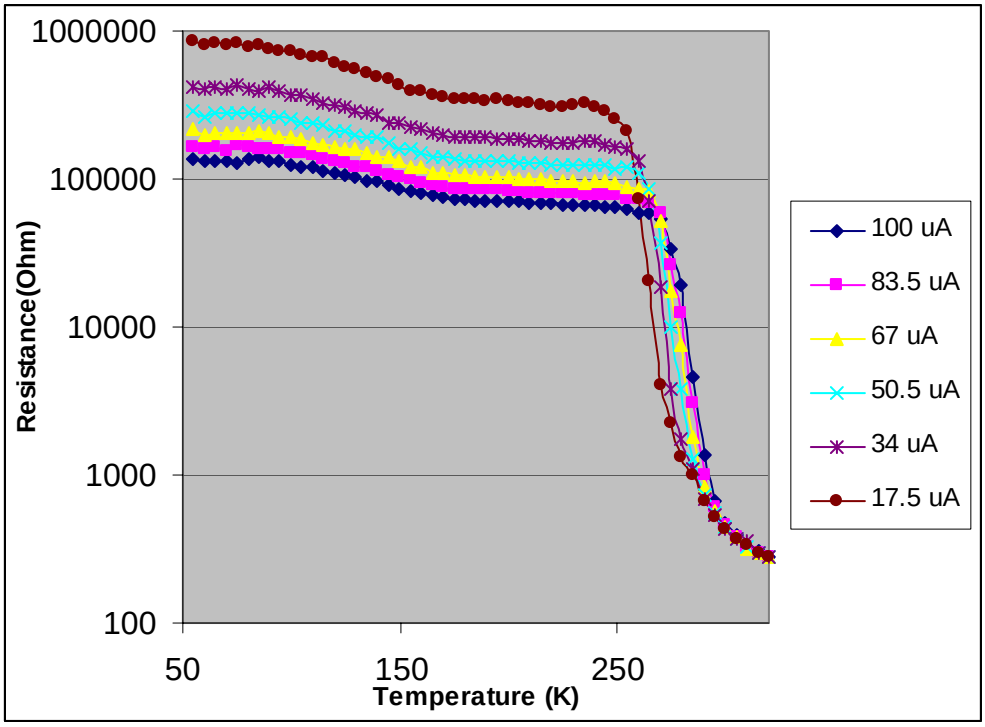

Figure 5.1.6 Temperature dependence of the resistance for discontinuous FeSi deposited film on *p*-type substrate

Figure5.1.5 also indicates that, as FeSi film is discontinuous, the only possible current path is through the substrate as shown by arrows. Temperatures dependant resistance measurements taken for discontinuous film is shown in the Figure 5.1.6. Low resistance of about 200 Ω could be observed in the temperature range of 320 K and 275 K and a transition similar to the one observed for the continuous film (Figure 5.1.1) was seen in the temperature range of 280 K and 250 K.

Due to the discontinuity of the film one can expect similar discontinuity in the inversion layer observed by Dai et al [J.Dai et al (2000)]. Results we observe clearly indicate a low resistive current path through highly resistive silicon oxide layer into the substrate by forming an Ohmic contact to the substrate at high temperatures.

This observation rules out the mechanism of current transport through the inversion layer at SiO_2/Si interface as described by Dai et all, instead the current transport is through the silicon substrate after tunneling through native SiO_2 layer.

To further probe the effect of the interface in the transition we have studied the isolated FeSi/SiO_2/Si junction. For this study the voltage probe were placed in the middle of the two junctions as shown in the Figure 5.1.7.the contact to Si was made by scratching the SiO_2 layer with a diamond scriber, followed by pressing indium contact. This method has been tested to give relatively good Ohmic contact to Si.

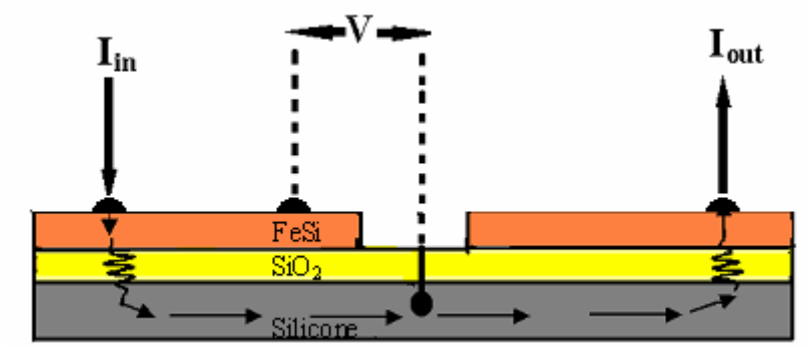

Figure 5.1.7 Schematic diagram of the voltage probe placement for isolated FeSi/Si interface.

Figure 5.1.8 shows the resistance dependence on temperature for one isolated $FeSi/SiO_2/Si$ (p-type) junction, which indicates a metallic behavior for both positive and negative current values until the transition temperature. With further decrease of the temperature graphs takes two different shapes for positive and negative current values passed through the sample. Three distinct transitions at 250 K, 220 K and 180 K can be clearly observed for the negative currents passed through the sample whereas for the positive currents values it displays usual transition discussed in the previous sections. For positive current, the current flows from FeSi film to Si while for negative current it flow from Si to FeSi film.

Resistance dependence on temperature was also tested for the isolated FeSi/Si system when deposited on *n*-type substrate following the same procedure discussed in the previous section. Interestingly, for the negative current values, usual metallic behavior during the 320 K and 280 K and the transition with four orders of magnitude is observed at 275 K as shown in the Figure 5.1.9 whereas for the positive current values, resistance decrease about 2 Ω with the decrease of the temperature down to 240 K and then starts to increase gradually with further decrease of the temperature from 240 K down to 50 K.

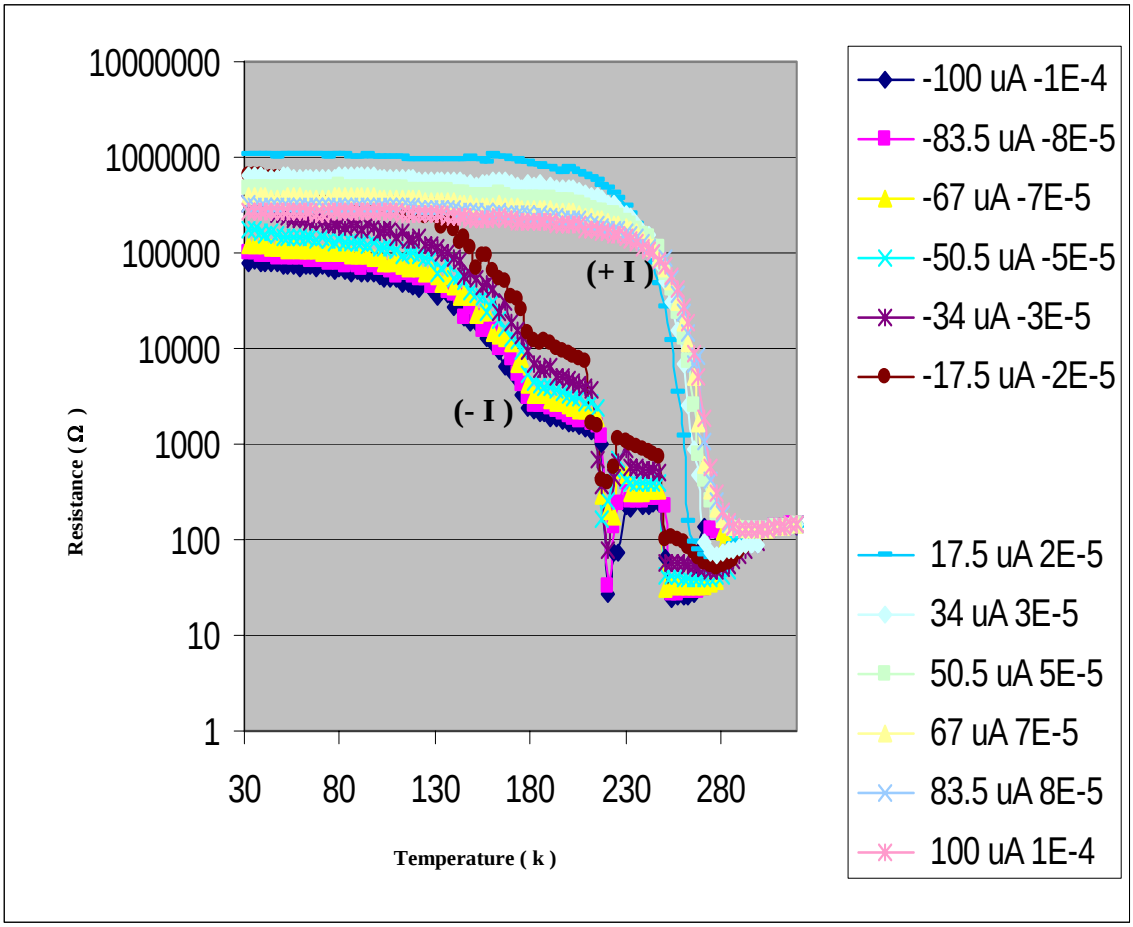

Figure 5.1.8 Temperature dependence of the resistance for an isolated FeSi/Si interface of a FeSi deposited film on *p*-type substrate.

It is noted that the usual transition around 265 K can be observed for isolated FeSi/ *p*-Si interface when current passes from the film to the substrate while the junction resistance remain low for current from Si to the film.

The data discussed in this section not only proves that the current flows through the substrate, but also illustrates that the transition we observe on FeSi deposited silicon

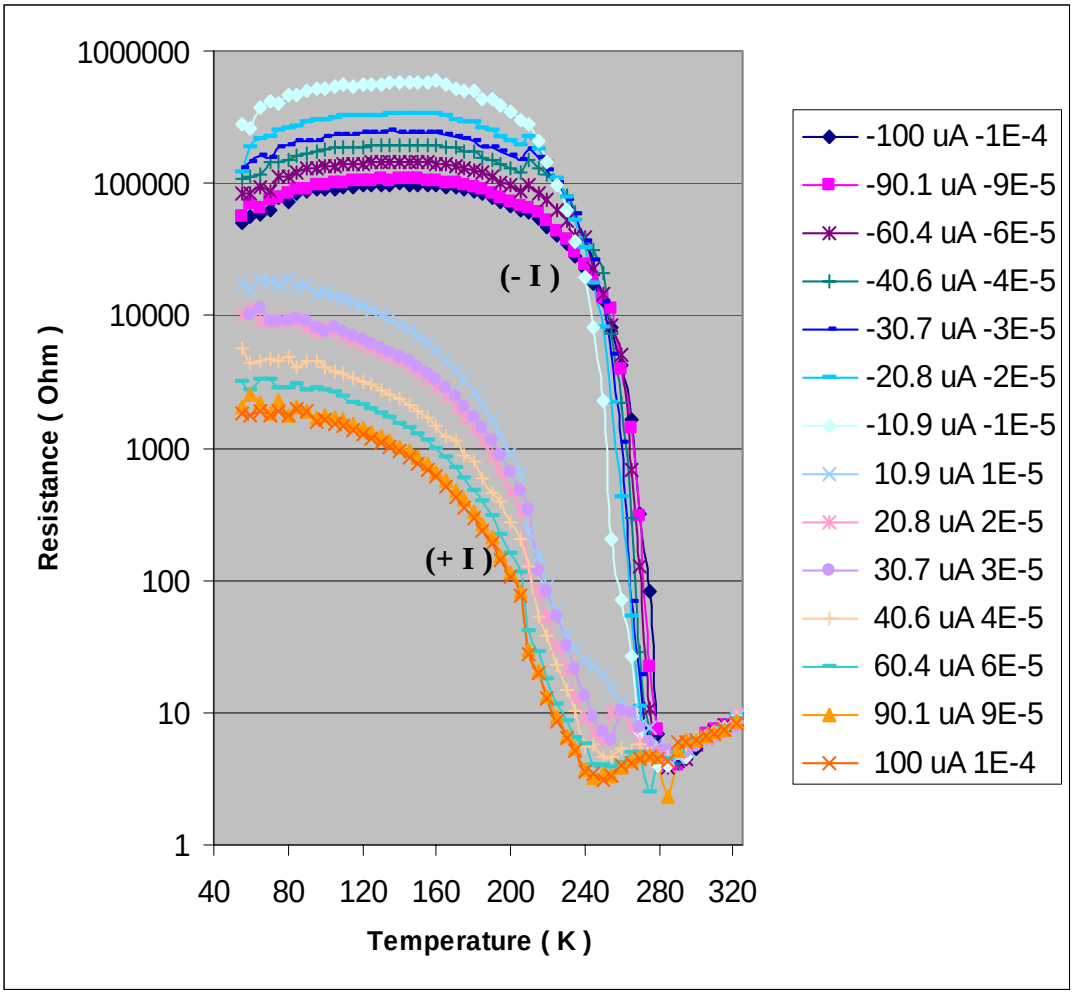

Figure 5.1.9 Temperature dependence of the resistance for an isolated FeSi/Si interface of a FeSi deposited film on *n*-type substrate.

substrates are due to the increase in the interfacial resistance of FeSi and silicon interface which depends on the direction of current. Summarizing the data in this section, after the transition temperature, lower resistance for the negative current values than the positive current values was observed for the FeSi films deposited on silicon *p*-type substrates, whereas resistance was higher for the for the negative current values .

5.2 Current-Voltage measurements (IV)

Forward and reverse bias characteristics of the isolated $FeSi/SiO_2/Si$ (p-type) junction (Figure 5.2.1) was investigated by IV measurements. Figure 5.2.1 shows the IV behavior at different temperatures. Linear relation was seen for the IV measurements taken for the temperatures higher than the transition temperature indicating metal like conduction mechanism and formation of an Ohmic contact with the substrate.

This system produced a non-linear relationship between current and voltage for forward and reverse bias directions in the temperature range where transition takes place

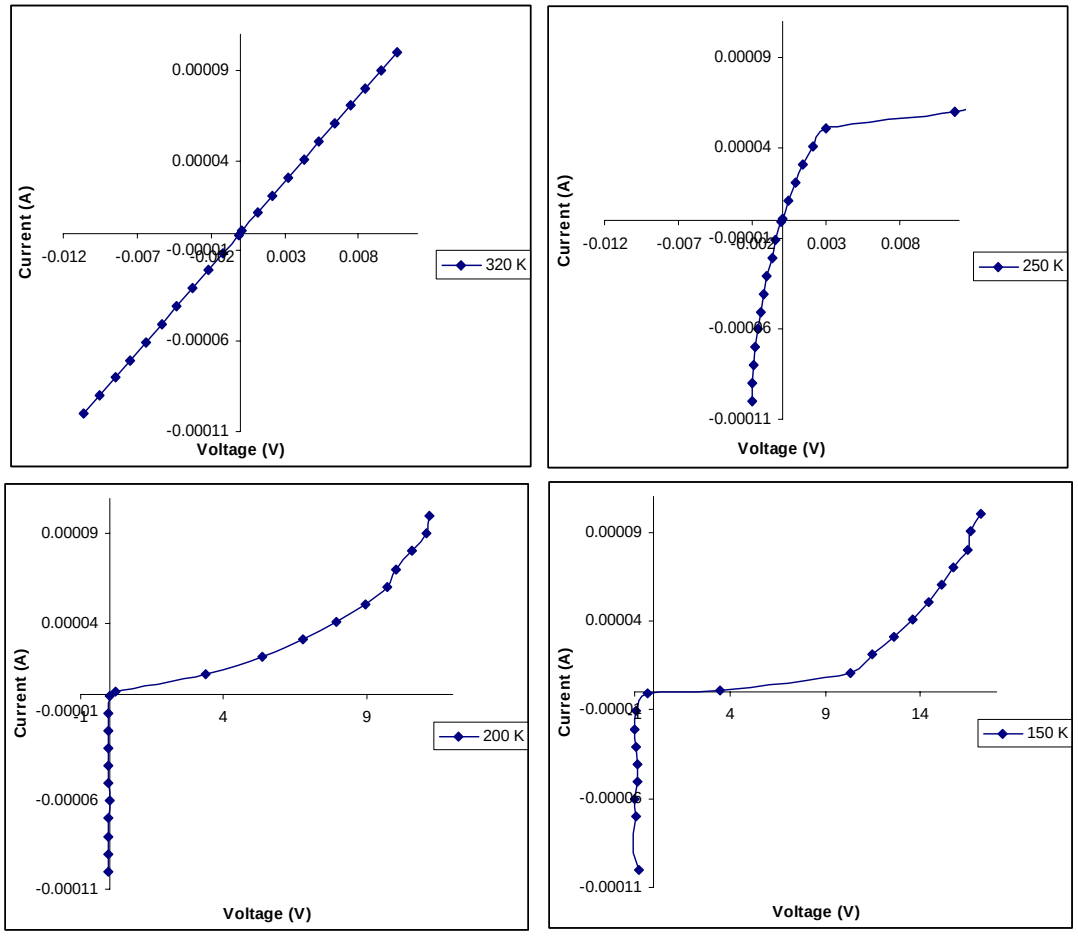

Figure 5.2.1 IV curves of an isolated $FeSi/SiO_2/Si$ (*p*-type) system taken at different temperatures

(260 K-230 K). Current-voltage measurements taken at 200 K indicate a behavior similar to that of a Zener diode, showing a Zener brake down in the negative direction of current. Interestingly this Zener breakdown voltage was gradually shifted to the left along the voltage axis for the IV measurements taken with further decrease of the temperature. Breakdown voltages of -0.9 V and –5 V were observed at 100 K and 50 K respectively.

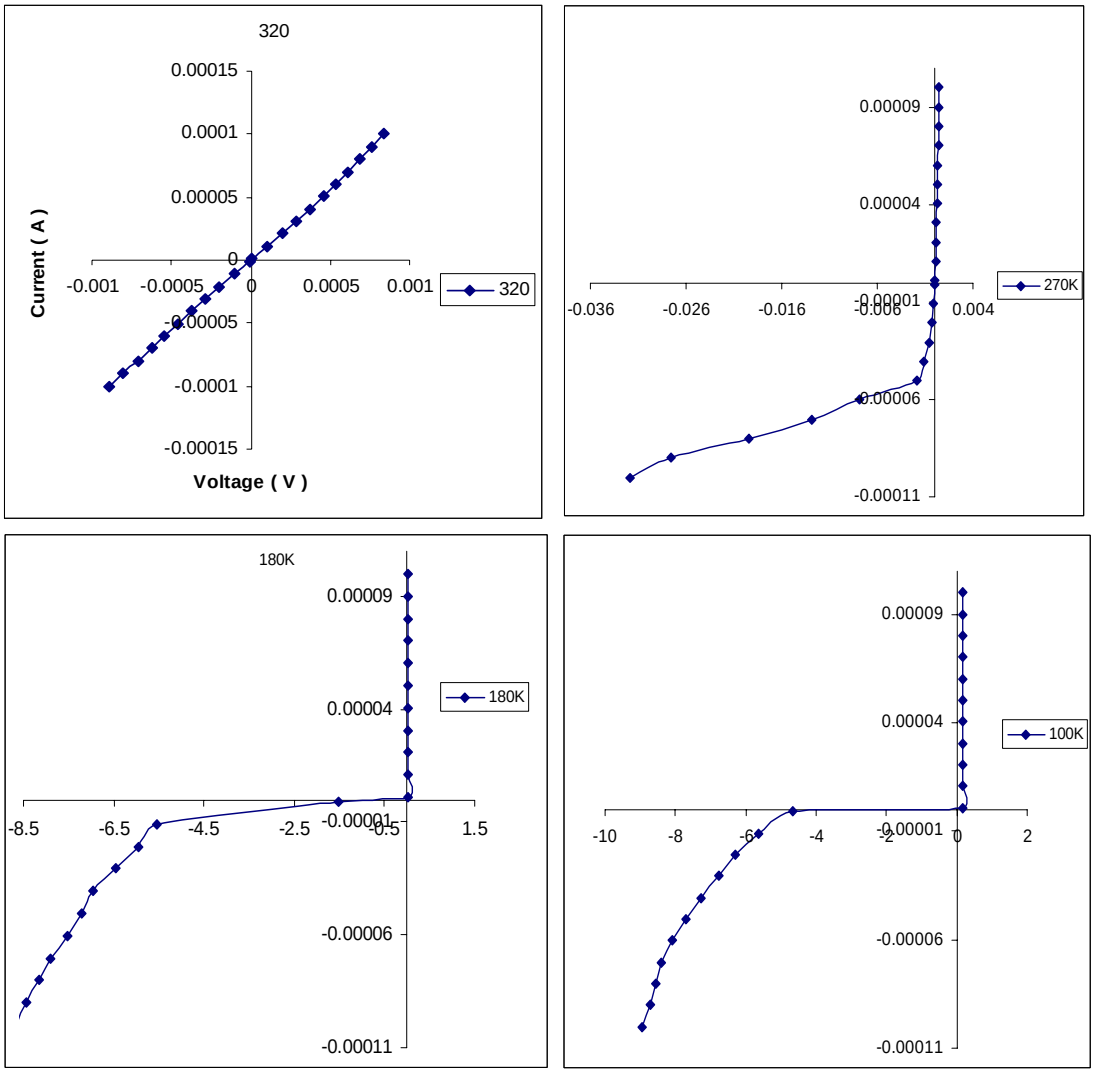

Figure 5.2.2 IV curves of an isolated FeSi/SiO_2/Si (*n*-type) system taken at different temperatures

Current-voltage measurements we obtained for isolated FeSi/SiO_2/Si (*n*-type) system at different temperatures are shown in Figure 5.2.2. These junctions showed a similar metallic behavior during the 320K down to 290K and a non-linear behavior for the IV curves taken bellow 280K. The IV behavior with positive current for a junction on *p*-type Si is similar to that observed with a negative current for a junction on *n*-type Si substrate.

5.3 Hall Voltage measurements

This section describes the Hall voltage measurements data collected on FeSi films deposited on *p*-type and *n*-type silicon substrates. The purpose of measuring the Hall voltage as a function of the temperature was to identifying the charge carrier type through the FeSi/SiO_2/Si interface.

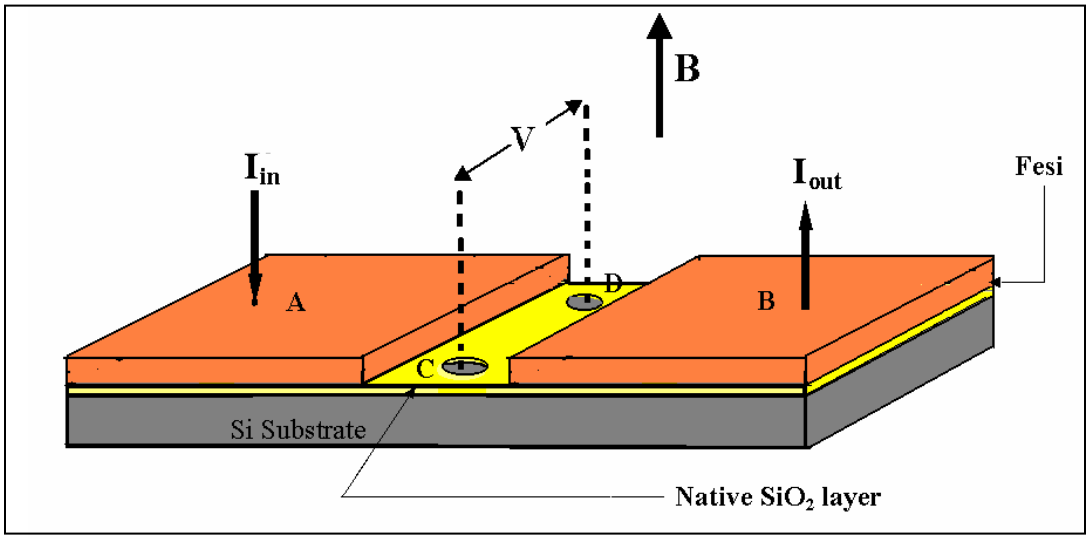

Figure 5.3.1 Schematic diagram of the current and voltage probe placement for Hall voltage measurements.

In this work a current was passed through points A and B and Voltage was measured between points C and D while placing a magnetic field in the perpendicular direction to the plane of the substrate as shown in the Figure 5.3.1. Points C and D were scratched to remove the SiO_2 layer using a diamond scribe to obtain a better contact with the substrate.

Hall voltage was measured by passing positive and negative currents of 200 mA and 137 mA in an applied magnetic field of 0.5 Tesla along both in and out directions

perpendicular to the plane of the substrate at every 10 K temperature deference. Final calculation for the Hall voltage was done as explained in the Chapter 4.

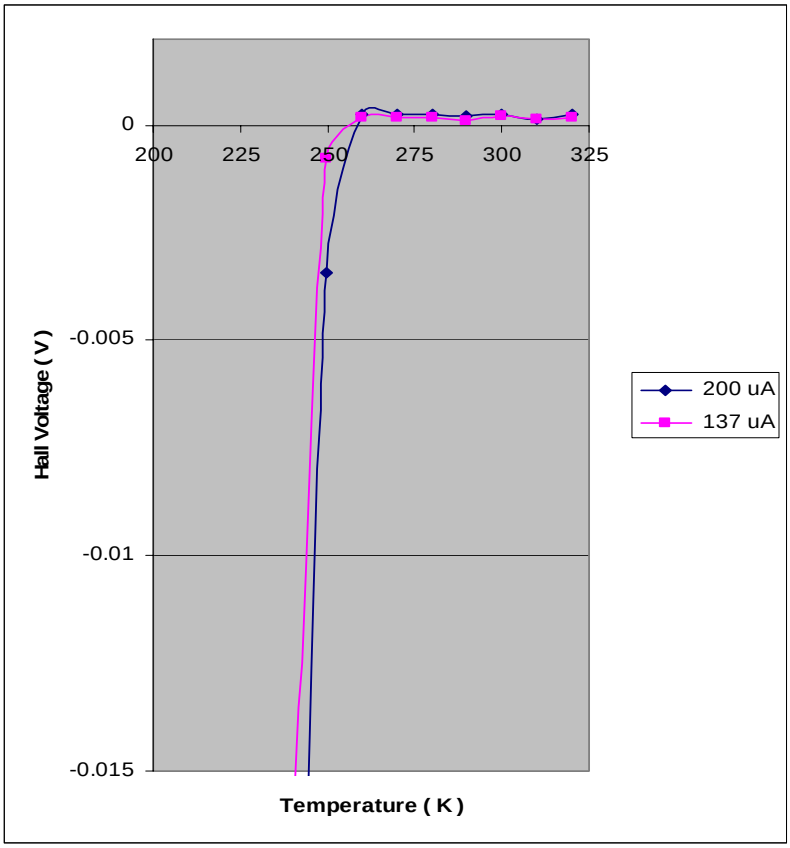

Figure 5.3.2 Hall voltage dependence on temperature for FeSi deposited on p-type silicon substrate measured for two different current values.

As the temperature decreased from 320 K a positive Hall voltage is observed until about 255 K. The observed hall voltage indicates “holes” which is considered as the majority carriers. Bellow 255 K hall coefficient changed from positive to negative that indicates electron transport. Then a rapid increase in negative voltage was observed as shown in the figure Figure5.3.2. Therefore, for current transport across a FeSi/SiO2/Si-p junction current transport is by “holes”, which are majority carriers down to 250 K and then changes to “electrons” as the temperature decreased beyond 250 K.

In the similar way, flipping of the sign in hall voltage from negative to positive could be observed at 230 K for the FeSi films deposited on n-type substrates. The data obtained or n-type substrates are shown in the Figure 3.3.3.

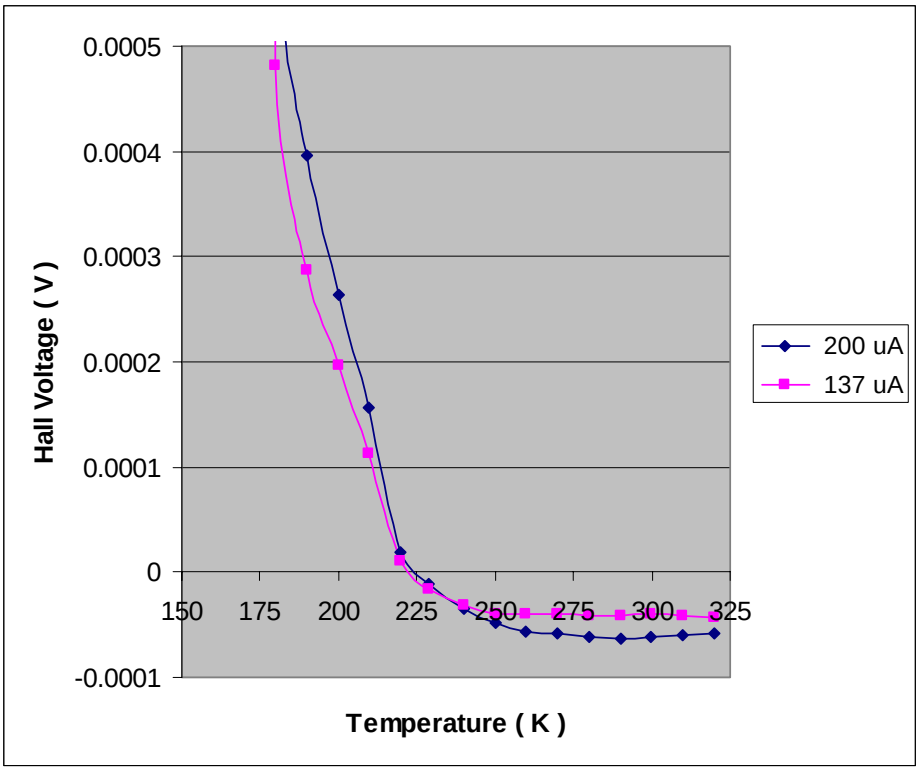

Figure 5.3.3 Hall voltage dependence on temperature for FeSi deposited on *n*-type silicon substrate measured for two different current values.

The rapid decrease in the Hall voltage in the Figure5.3.3 indicates that there has been a rapid drop in the carrier density as temperature dropped bellow 255K. Similar characteristics can be seen in the figure bellow 230K. Alteration of the sign in the Hall voltage, at 255K can be well matched with the transition observed in the FeSi deposited on the p-type substrate. However transition temperature observed on n-type substrates was not as same as the temperature at which the Hall voltage flips from negative to positive in the Figure 5.3.3.

Finally it could be found that carrier type through the FeSi/Si interface changes from majority to minority carriers at 255 K and 230 K respectively for *p*-type and *n*-type substrates as the temperature decreases.

5.4 Metal/FeSi/SiO_2/Si junctions

In order to understand the effect of the presence of magnetic ion Fe in the transition behavior, discontinuous FeSi films grown on *p*-type Si substrate were compared with the discontinuous non-magnetic metals such as platinum (Pt) and aluminum (Al). The structures of interest for this study were Pt/SiO_2/*p*-Si and Pt/FeSi/SiO_2/*p*-Si. As shown in Figure.5.4.1, a discontinuous FeSi film was deposited by placing a mask in the middle of the substrate. Thickness of the FeSi film was about 50 nm. Following FeSi growth, 20 nm thick platinum metal layer was sputtered top of the FeSi film. Resistance dependence on temperature was tested for the systems of Pt/FeSi/SiO_2/Si-*p* and Pt/SiO_2/Si-*p*.

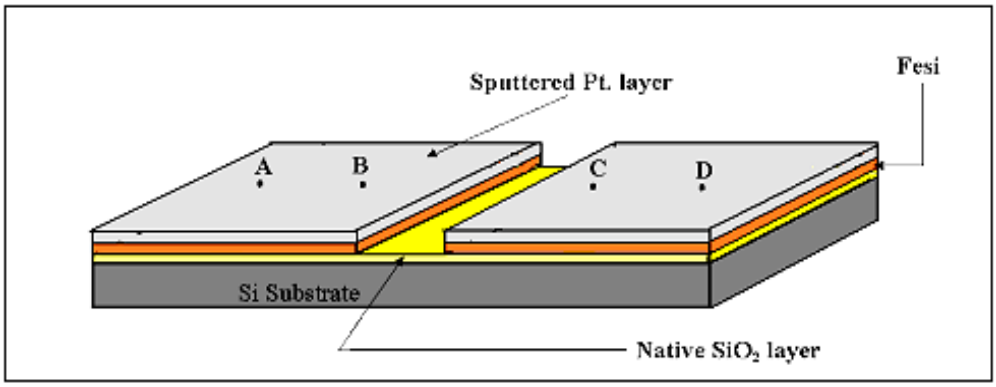

Figure 5.4.1 Schematic diagram of the fabrication procedure of FeSi films with sputtered platinum layer.

As seen in Figure 5.4.2 the current transport across the Pt/SiO_2 layer encountered a high resistance, such as in a shottkey diode. This resistance continued to increase with decreasing temperature. However, the presence of ultra thin FeSi layer produced an ohmic contact between Pt and *p*-Si substrate across the SiO_2 layer. In addition, metal-to-

insulator transition observed for a FeSi film was also observed for this structure as shown in the Figure 5.4.3.

The need of magnetic material to observe this transition was further reinforced in the Al/SiO_2/*p*-Si and Al/FeSi/SiO_2/*p*-Si structures. A 4.5 μm thick Al layer was coated on the Si and FeSi/Si using an electron beam evaporator. We performed the electrical measurements for different current values as discussed in the previous sections. The resultant data are presented, respectively, for Al/Si and Al/FeSi/Si, in Figure 5.4.4 Basically, the results are analogous as those of the metallic schemes prepared using Pt (Pt/Si and Pt/FeSi/Si).

In the case of Al/FeSi/ SiO_2/*p*-Si structures, the resistance did not increase until the temperature reaches 290 K. Following this transition point the resistance increased rapidly until 250K, followed by a gradual increase up to 0.2 MΩ with further decrease of the temperature. On the other hand, for the Al/Si scheme, no such transition in the resistance is observed, obviously confirming that FeSi plays a key role in transition. In overall, our experimental results suggest that transition observed for discontinuous FeSi/Si scheme cannot be obtained for the discontinuous non-magnetic metal coated on the same Si substrates

Additionally, further studies were carried with discontinuous Aluminum coated *p*-type silicon substrates by annealing the sample at 400 ^{o}C for 30 minutes in 2.3x10^{-6} T vacuum.

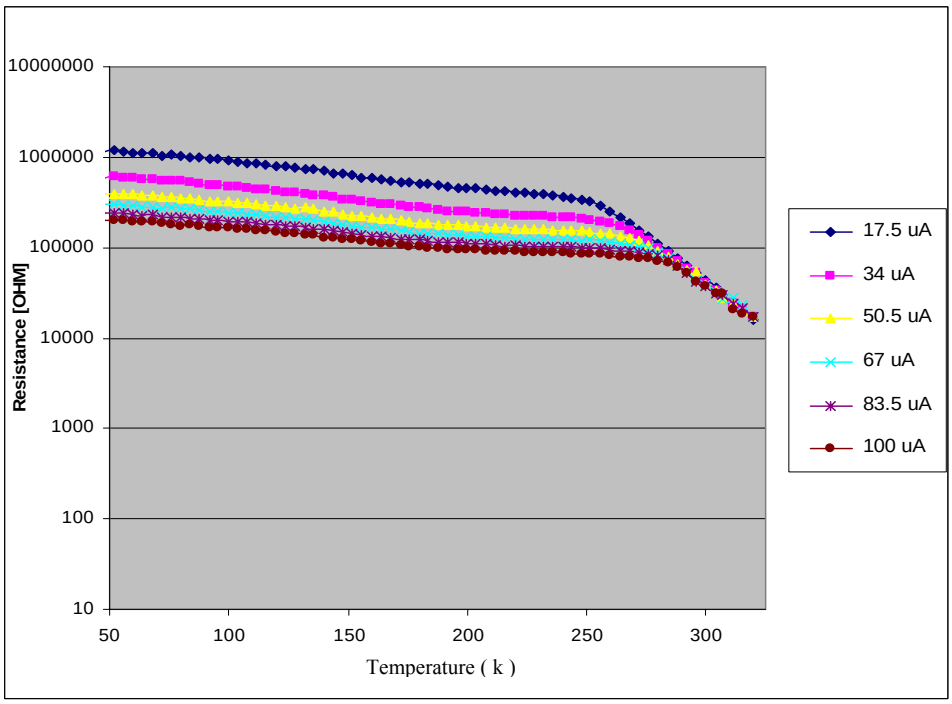

Figure 5.4.2 The resistance dependence on temperature of and Pt/SiO_2/Si-*p* structure

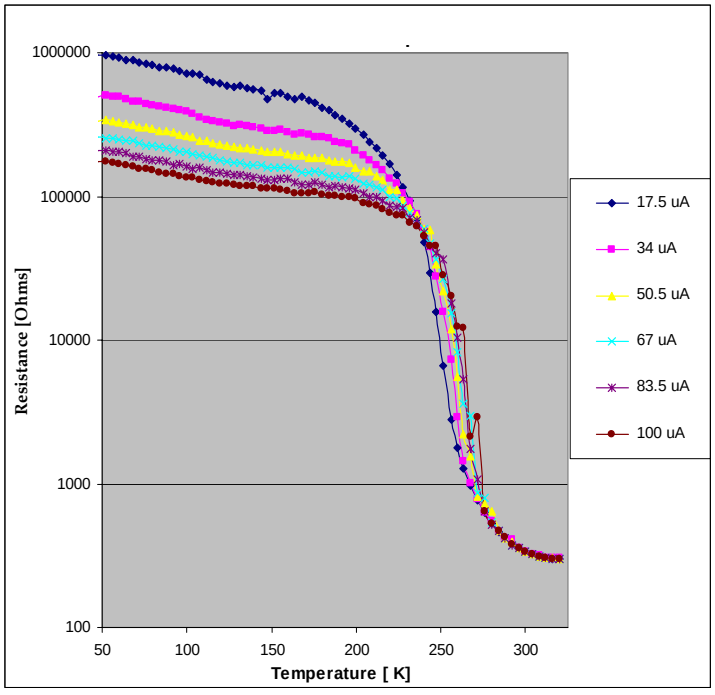

Figure 5.4.3 The resistance dependence on temperature of and Pt/FeSi/SiO_2/Si-*p* structure

The Resistance dependence on temperature for the annealed Al/SiO_2/*p*-Si is shown in Figure 5.4.5. This shows an enormous Resistance drop down to about 200Ω when compared with values in the Figure 5.4.4. As the temperature decreased, resistance linearly decreases down to 100K and then rapidly increases with further decrease of the temperature. Similar behavior was seen in the temperature depending resistivity curve for the Boron doped Silicon substrates explained in the figure 3.2.2 in the section 3.2. Therefore, it is clear that by annealing the film, Al is diffused through the SiO_2 layer to make an ohmic contact for all temperatures.

Voltage Vs current (IV) data obtained at different temperatures is shown in the Figure 5.4.6. Interestingly this Ohmic behavior is seen throughout the temperature range between 320 K and 40 K. Overlaying of two resistance curves measured for 1 μA and 100 μA in the Figure 5.4.5 also shows the linear behavior observed in the IV curves.

Note that this process of annealed Aluminum coating was directly used in forming Ohmic contacts with the Si substrate for the further studies of the FeSi/Si interface discussed in this thesis.

From the observed results, it is evident that, there has been a diffusion of Aluminum through highly insulating, native Silicon Oxide layer and Aluminum coating has formed a perfect Ohmic contact with the substrate during the process of annealing. Based on this one can expect diffusion of magnetic Fe ion occurs through the highly oxide layer and forms an Ohmic contact with the substrate. However, in presence of a magnetic element such as Fe, Localization of electrons takes place around 250 K that leads to a metal-to-insulator transition.

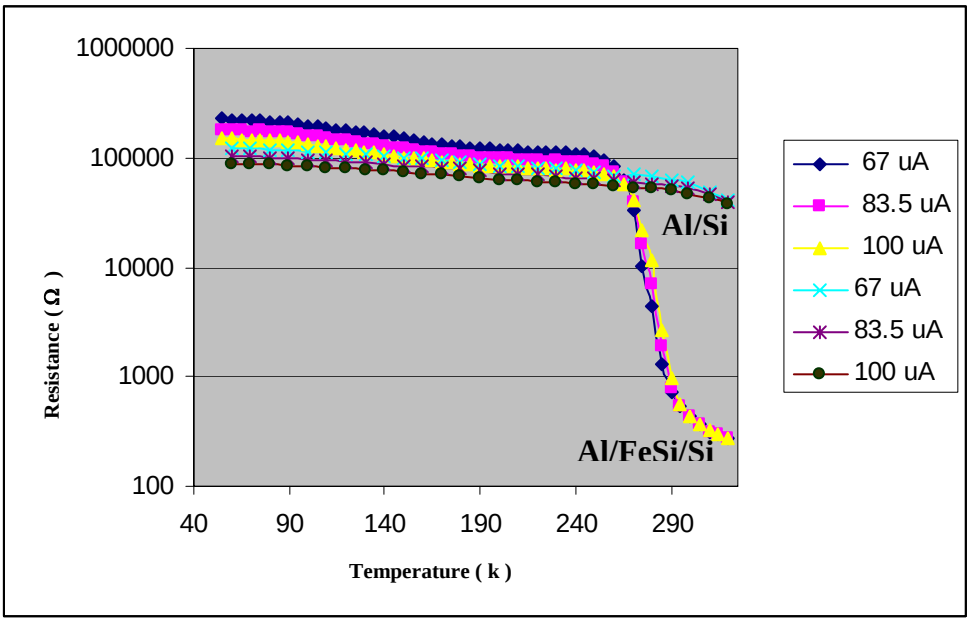

Figure 5.4.4 The temperature dependence of resistance of discontinuous Aluminum coated and Aluminum coated FeSi deposited films on silicon substrates.

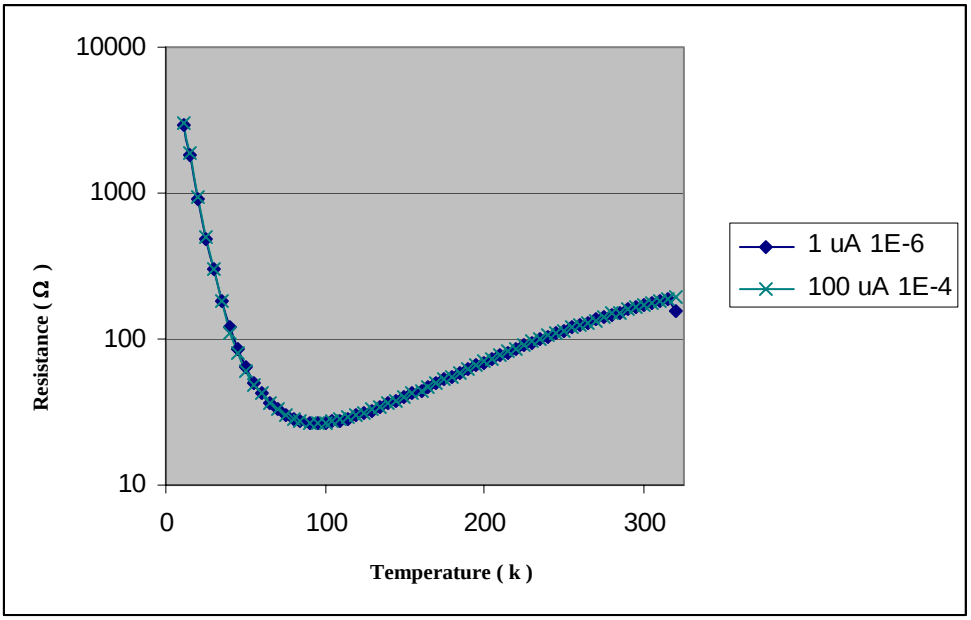

Figure 5.4.5 The temperature dependence of resistance of discontinuous Aluminum coated after annealing at 450 ^{0}C for 30 minutes.

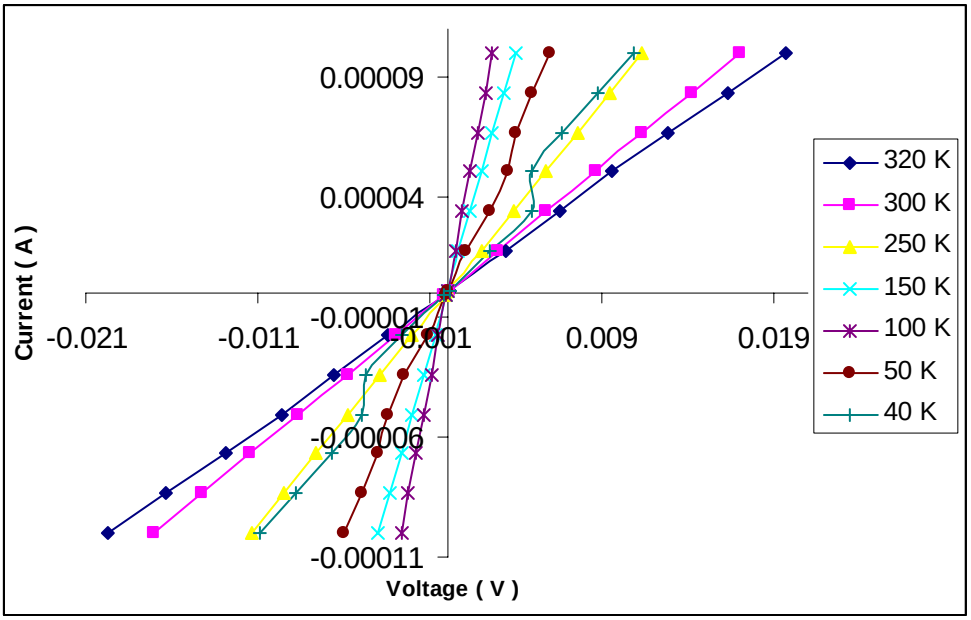

Figure 5.4.6 IV curves of annealed discontinuous Al/Si system taken at different temperatures

Summery:

Following observations were made in the electrical characterization of FeSi films

1) Four order of magnitude change in the resistance was observed at 250 K and 300 K for the continuous FeSi deposited on *p*-type and *n*-type silicon substrates. Similar transition was obtained for the discontinuous FeSi films deposited on silicon substrates. This confirms that the current transport is not confined to an inversion layer at the SiO_2/Si interface.

2) Resistance measurements taken for isolated FeSi/ SiO_2/Si systems indicated a metallic behavior down to the transition temperature followed by a metal-to-insulator transition around 250K. After the transition temperature the junction showed a lower resistance for negative currents while the positive currents

produced a higher junction resistance for *p*-type substrate. The opposite effect was observed for *n*-type Si substrates.

3) Resistance dependence studied on discontinuous Pt and Al metallic films did not show an Ohmic contact to the Si substrate. Furthermore, diffusion of Al b annealing the Al contact that was deposited directly on substrate (no FeSi film) produced an Ohmic contact down to low temperature with out the metal-to-insulator transition. However an ultra thin FeSi layer between the metal and substrate produced an Ohmic contact at room temperature around 250 K.

Chapter 6

Fluence Dependence on Transition and Ion probe studies

6.1 Laser fluence dependence on transition

Laser energy per unit area is defined as the laser fluence (J/cm^2). Higher the laser fluence, higher the energy of the ablated species. An experiment was performed to identify the effect of the laser fluence on the transition observed in FeSi films on Si substrates. This study involved nine different FeSi films those were deposited using nine different laser fluences.

Laser fluence was controlled by, changing the spot size on the target and energy of the laser pulses. Number of shots were decreased with increasing laser fluence to keep the thickness of the samples same. Burn pattern for 10 shots of the laser beam on a photographic paper was taken and area was calculated by measuring the dimensions of the burn pattern. Table 6.1.1 illustrates the different parameters used during the deposition.

Figure 6.1.1a and 6.1.1b, show that resistance vs. temperature measurements for two current values of the films deposited at nine different fluences.(1 μA and 100 μA). The highest magnitude of the transition with four orders of magnitude of change was obtained for the FeSi films deposited with 0.64 J/cm^2 laser fluence whereas the transition with a lowest magnitude of 10 Ω was observed when deposited with 3.83 J/cm^2. As seen in these figures, the resistances of the FeSi samples below the transition temperature is dramatically reduced with increasing laser fluence. The effect of probe current is also

more pronounced for films deposited at low fluence. A drop in the resistance, even in the region where metallic behavior is observed (320 K down to 250 K), can also be seen with the increase of the laser fluence.

Sample No	**Repetition Rate (Hz)**	**No. of Shots**	**Laser Energy (mJ)**	**Laser Spot Size (cm^2)**	**Laser Fluence (J/cm^2)**
1	10	35000	45	0.070	**0.64**
2	10	25000	45	0.058	**0.78**
3	10	18000	45	0.041	**1.10**
4	10	9000	90	0.057	**1.58**
5	10	6000	135	0.079	**1.71**
6	10	4500	170	0.088	**1.93**
7	10	3500	230	0.092	**2.50**
8	10	3250	230	0.065	**3.53**
9	10	3000	230	0.060	**3.83**

Table 6.1.1 different parameters used during the deposition

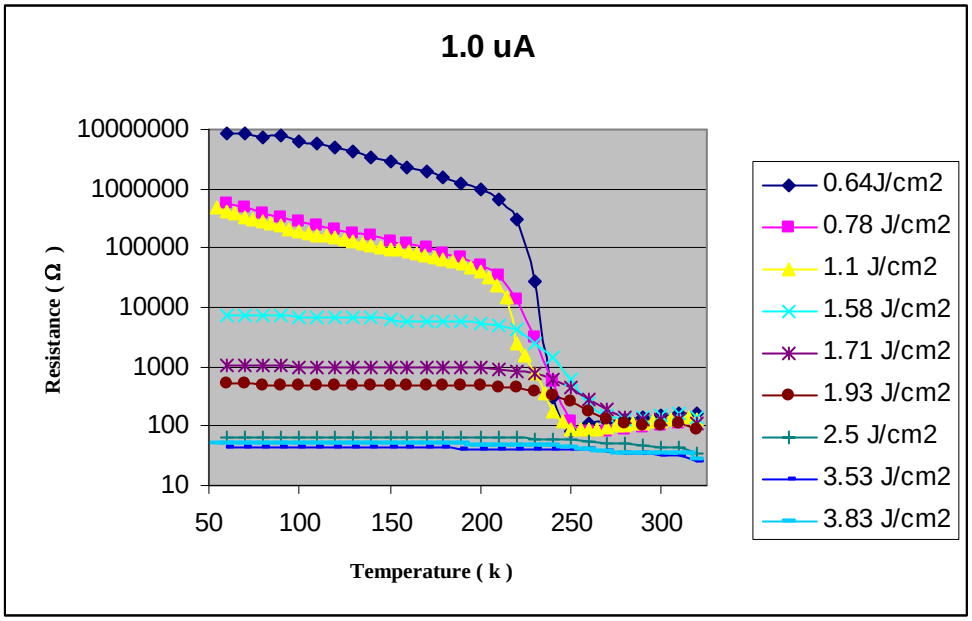

(a)

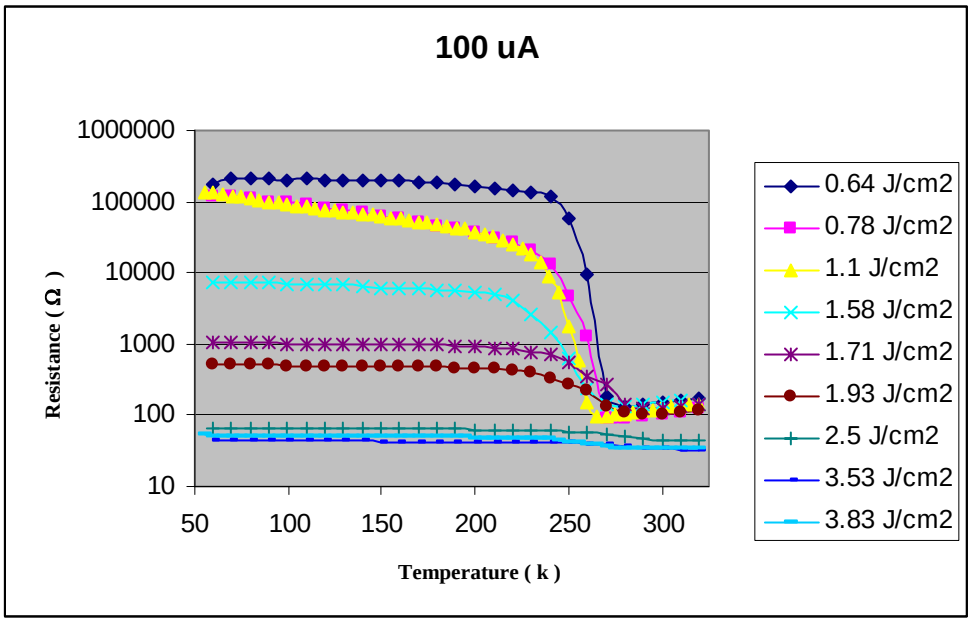

(b)

Figure 6.1.1 Transition magnitude dependence on laser fluence for FeSi deposited on p-type silicon substrate measured for two different current values (a) 1 µA (b) 100 µA

6.2 IV Characteristics

Current as a function of the voltage (IV) at different temperatures, were measured for the samples described in the table 6.1.1. Figure 6.2.1 indicates the some of the IV data obtained (for temperatures of 300, 250, 240, 200, 100 and 60 K), for the FeSi films deposited with 0.71 J/cm^2 laser fluence. IV plots exhibit a linear relation from 320 K down to the transition point and a non-linear behavior from 260 K down to 50 K for all the samples deposited with lower fluence (< 1.10 J/cm^2). For the samples deposited with medium laser fluence this non-linear behavior was only observed during the transition temperature as shown in the Figure 6.2.2 a. However a linear relationship in all the IV curves was observed for the samples deposited with higher laser fluence (>2.5 J/cm^2) through out the temperature range between 320 K and 50 K. Figure 6.2.2 b illustrates the IV data obtained for the FeSi films deposited with laser fluence of 3.5 J/cm^2.

Finally, these IV measurements indicate that materials form an ohmic contact, where the current and voltage obeys Ohm's law and the resistance is just the reciprocal of the slope of a straight line in a V *versus* I curve throughout the temperature range of 320 K down to 50 K when films are deposited with laser fluence higher than 2.5 J/cm^2.

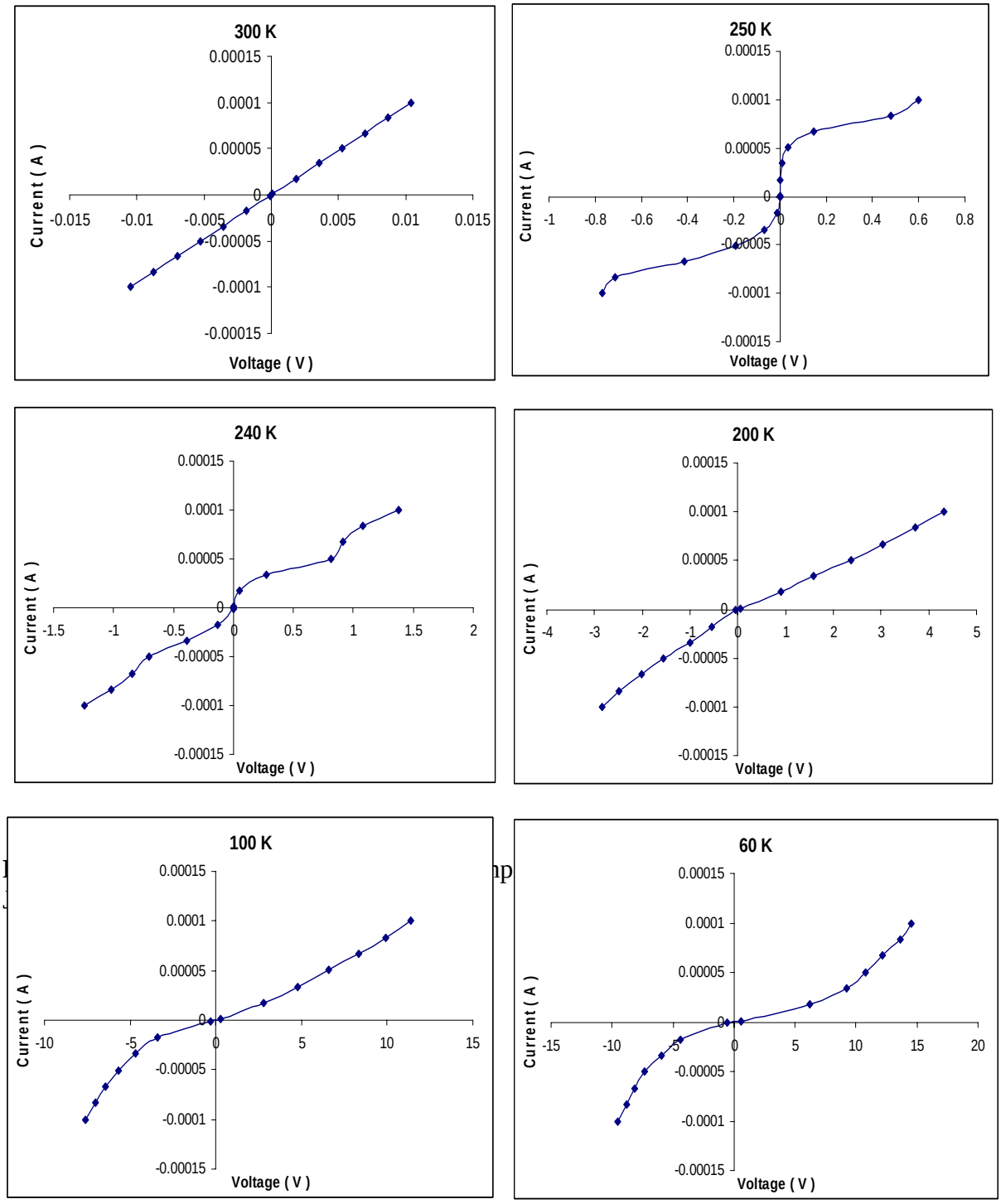

Figure 6.2.1 IV characteristics at different temperatures of FeSi film deposited with 0.71 J/cm^2 laser fluence

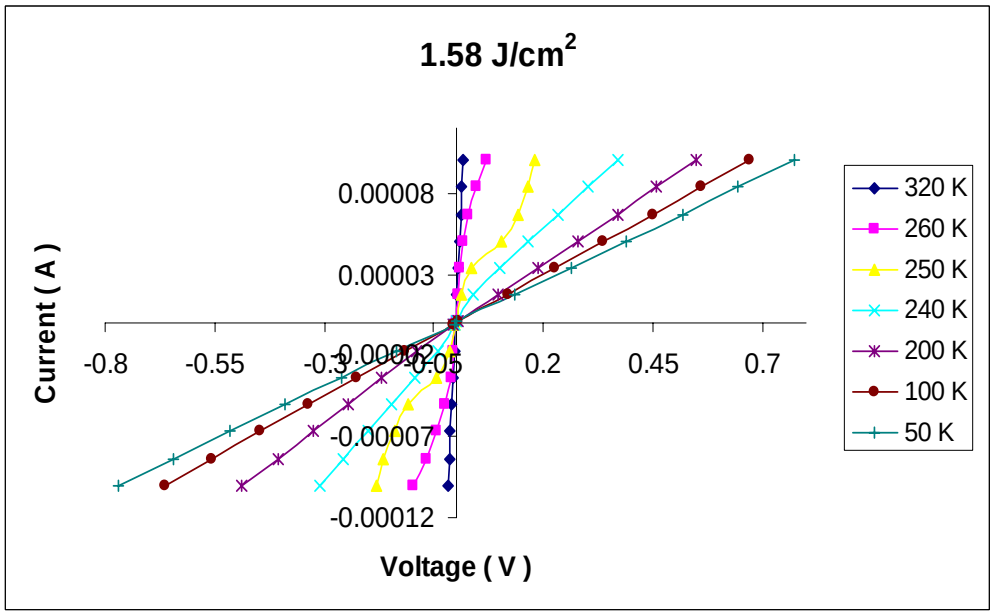

(a)

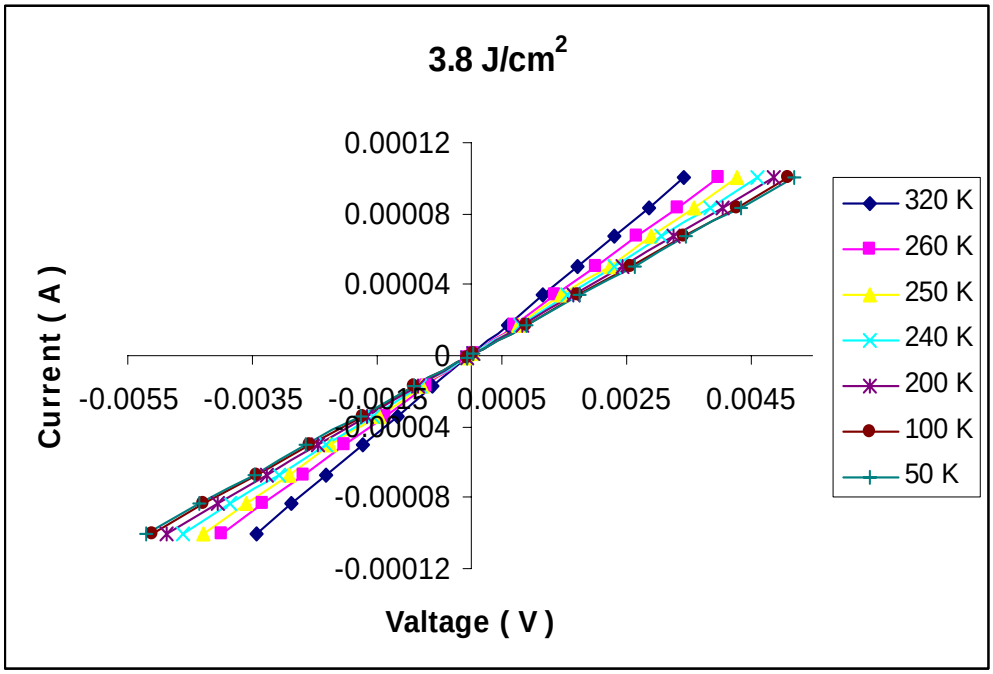

(b)

Figure 6.2.2 IV characteristics at different temperatures of FeSi film deposited with (a) 1.58 J/cm^2 and (b) 3.8 J/cm^2 laser fluence

6.3 Investigations with Ion Probe.

Since change in the fluence affected the transition magnitude, it was our interest to carry out a set of experiments to understand the reasons for such behavior. Since increasing fluence gives rise to high species energy, at high fluences the energy of the Fe atoms and ions strike the substrate with higher velocity. To measure the energy of the ions produced by laser ablation an ion probe measurement was carried out.

Time-of-flight ion probe measurements can be used to obtain information on ionic content and the velocity distribution of the plasma species. The probe used for this technique is simply a metal wire or a disc that is in contact with the plasma; typically a probe with a small cross sectional area is used to minimize the perturbation of the plasma plume. This section presents the results of the experiments carried out to determine the effect of various process parameters in the ionic contacts in the plasma plume created in different laser energies and their effect on the metal-to-insulator transition.

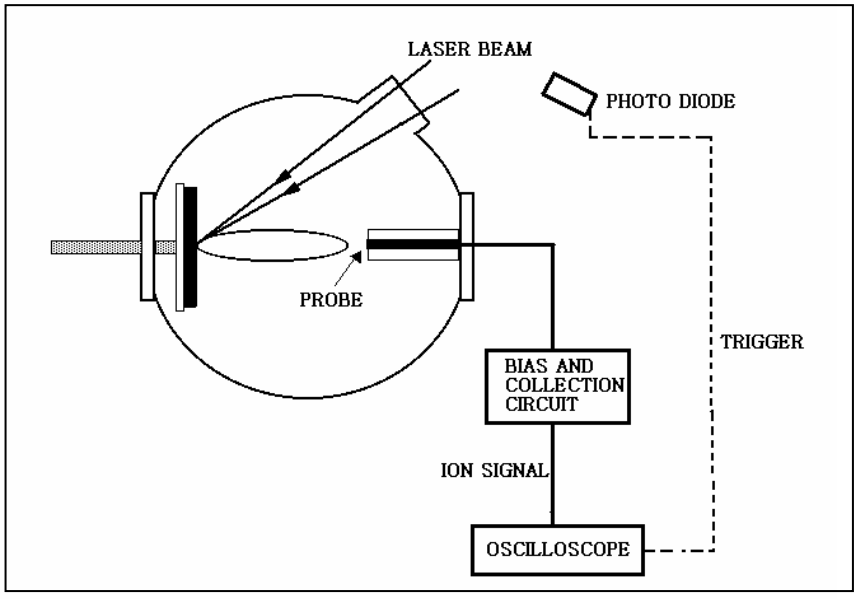

Figure 6.3.1 schematic diagram of the ion probe set up.

Ion probe was constructed by smoothening the edge of a 14 gauge insulated copper wire. The calculated cross sectional area of the probe was 2.164mm^2. Probe was then connected to an oscilloscope through the bias and the collection circuit (Figure6.3.2) as shown in the figure 6.3.1. A negative bias voltage of 18V was applied in order to attract positive ions towards the ion probe and repel elections away from the ion probe. The Signal coming out of the bias circuit was connected to the channel-2 input of the oscilloscope and the signal coming from the UV detector was directly connected to the channel-1 input of the oscilloscope. Two 50Ω terminators were used at both the channels to match the line impedance of probe and the sensor.

Mounting the ion probe on axis of the plume, 4cm away from the target and facing the plum directly, ion signals and the laser signals were simultaneously monitored on the oscilloscope screen.

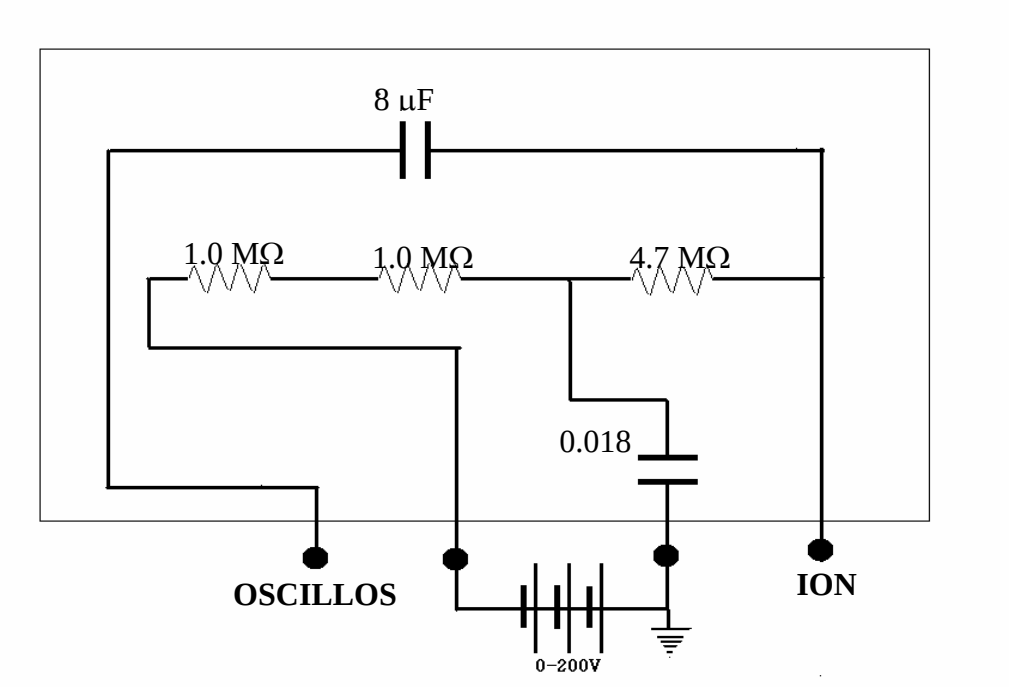

Figure 6.3.2 Bias and collecting circuit used

The fluence was changed by changing the laser energy and ion probe signal for each distinct fluence was recorded in the oscilloscope after averaging with 64 data sets. Transient time-of-flight ion profiles obtained at different fluences are shown in the figure 6.3.3

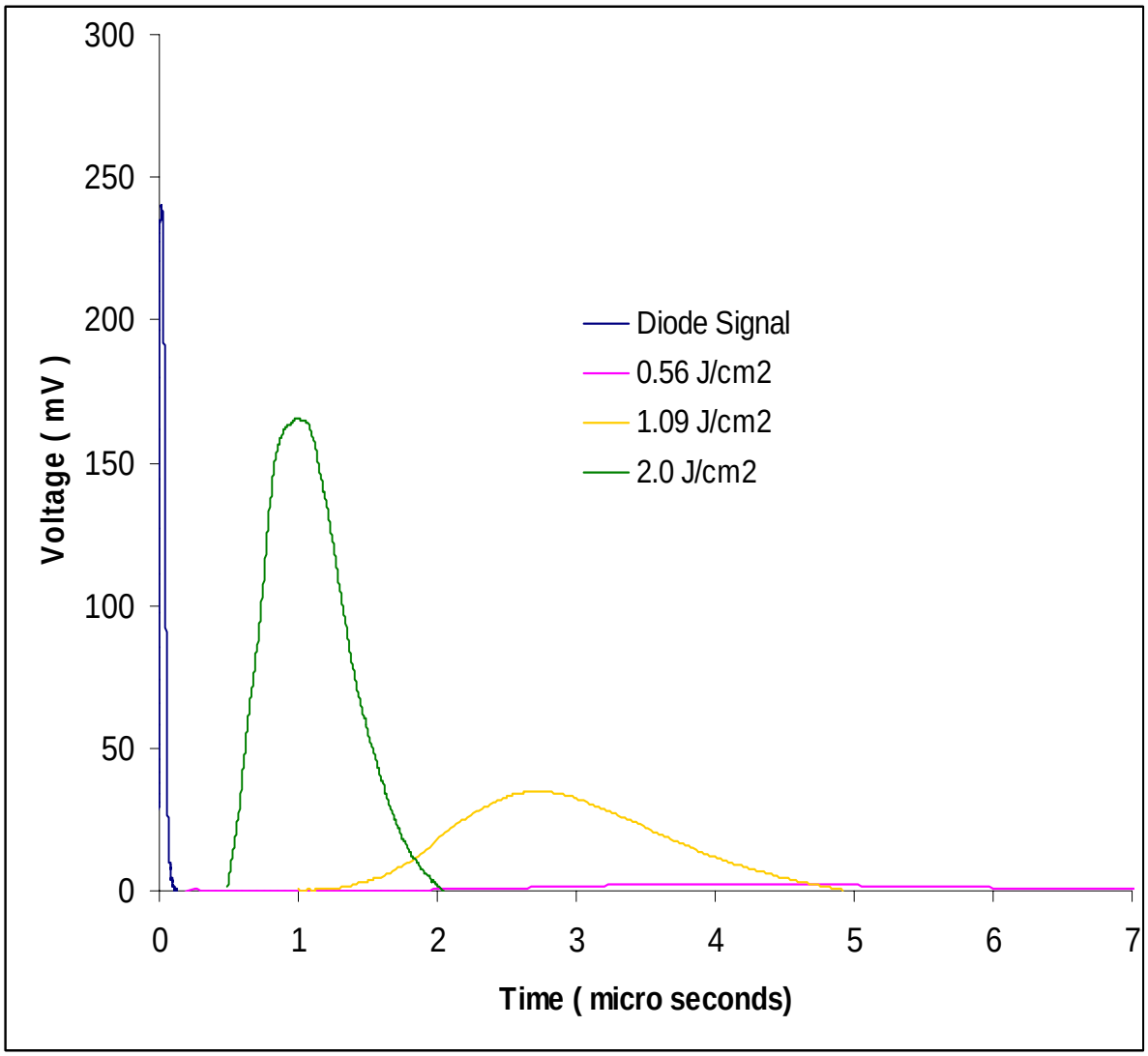

Figure 6.3.3 The diode signal and the time-of-flight ion profiles obtained at different laser fluences.

The density of ions, which corresponds to the area under the curve of time-of-flight profiles, was obtained by integrating the area under the curve over the duration of the profile and plotted against laser fluences (Figure 6.3.4). Time-of-flight was calculated from peak to peak time difference of the laser signal and the ion signal and then plotted against the Fluence (Figure 6.3.5)..

Average velocity of ions was calculated by dividing the distance between the target by the time-of-flight. The average Energy of Fe ions was calculated using the most probable velocity of ions. (Figures 6.3.6 and 6.3.7). Increase of the kinetic energy of the Fe ion as the fluence is increased can be clearly seen in the figure 7.2.7.

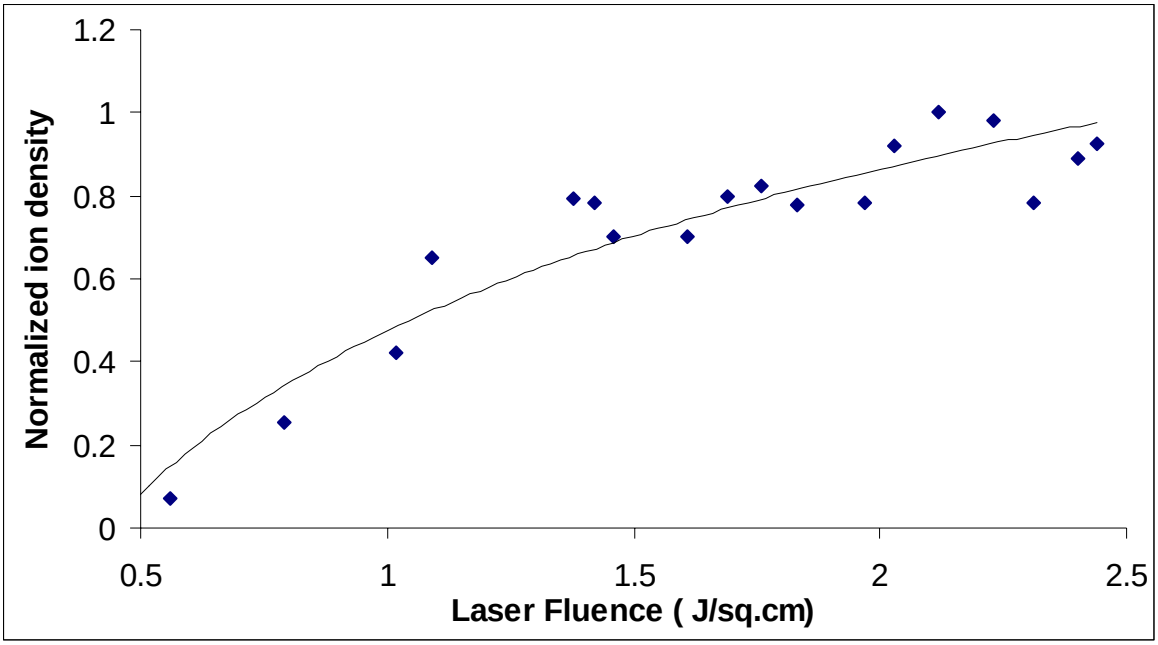

Figure 6.3.4 Fluence dependence of Normalized ion density.

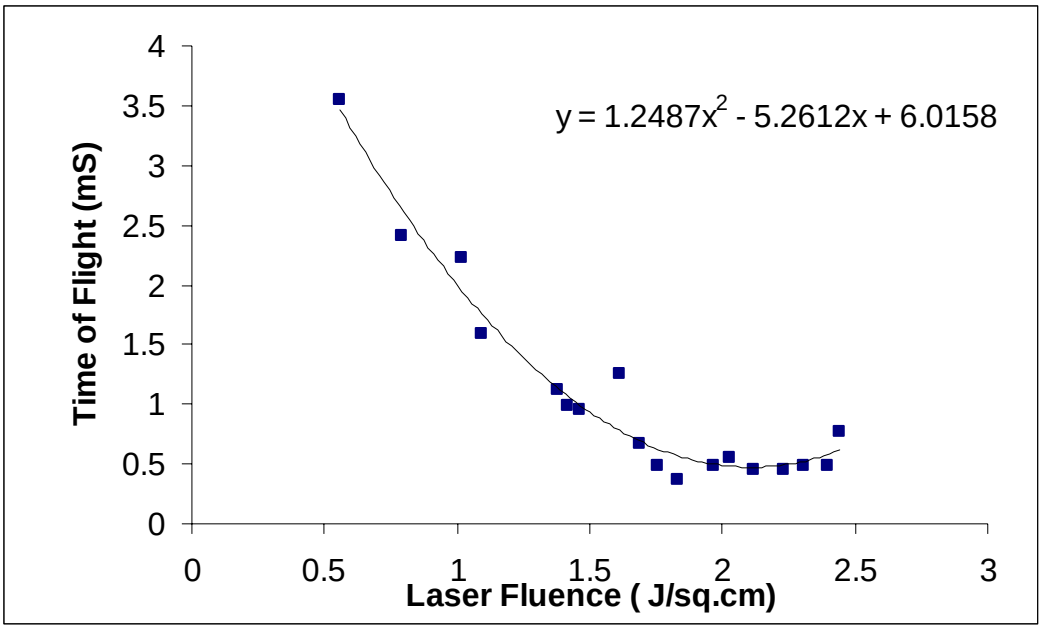

Figure 6.3.5 Fluence dependence of time-of-flight

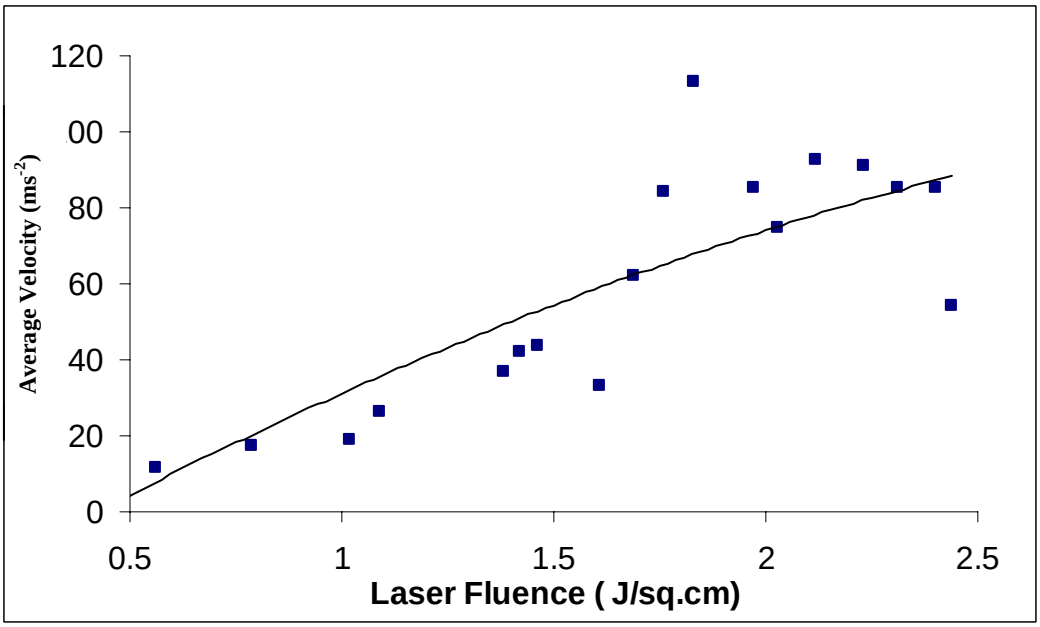

Figure 6.3.6 Fluence dependence of average velocity of the ion.

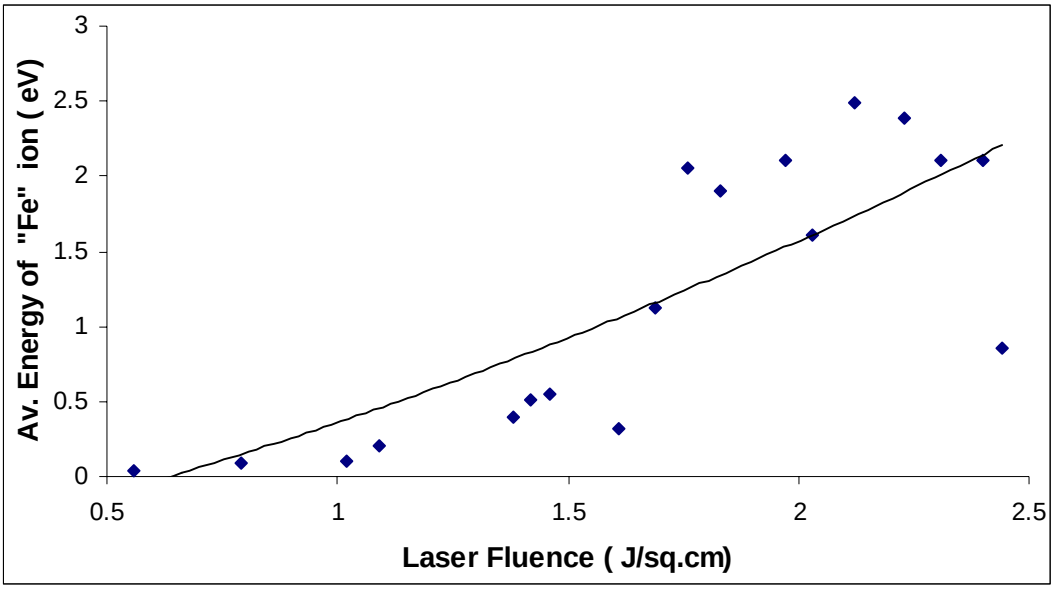

Figure 6.3.7 Fluence dependence of average Energy of “Fe” ions.

Clearly the observed effect of laser fluence on the transport properties has a great influence from the increase in the kinetic energy of Fe atoms and ions.

6.4 Thickness Dependence on Transition.

Next interest was to find the effect on the thickness of the film on the transition. This was tested for films deposited both at high fluence and lower fluence. Two films at low fluence and four in high fluence were deposited with different thickness. Number of shots was counted and finally thickness per a shot was calculated measuring the thickness of the thickest films in two sets of samples using a profilometer described in the chapter 4. Thicknesses of other samples were calculated by multiplying the thickness per shot at that fluence with the number of shots of the deposited film.

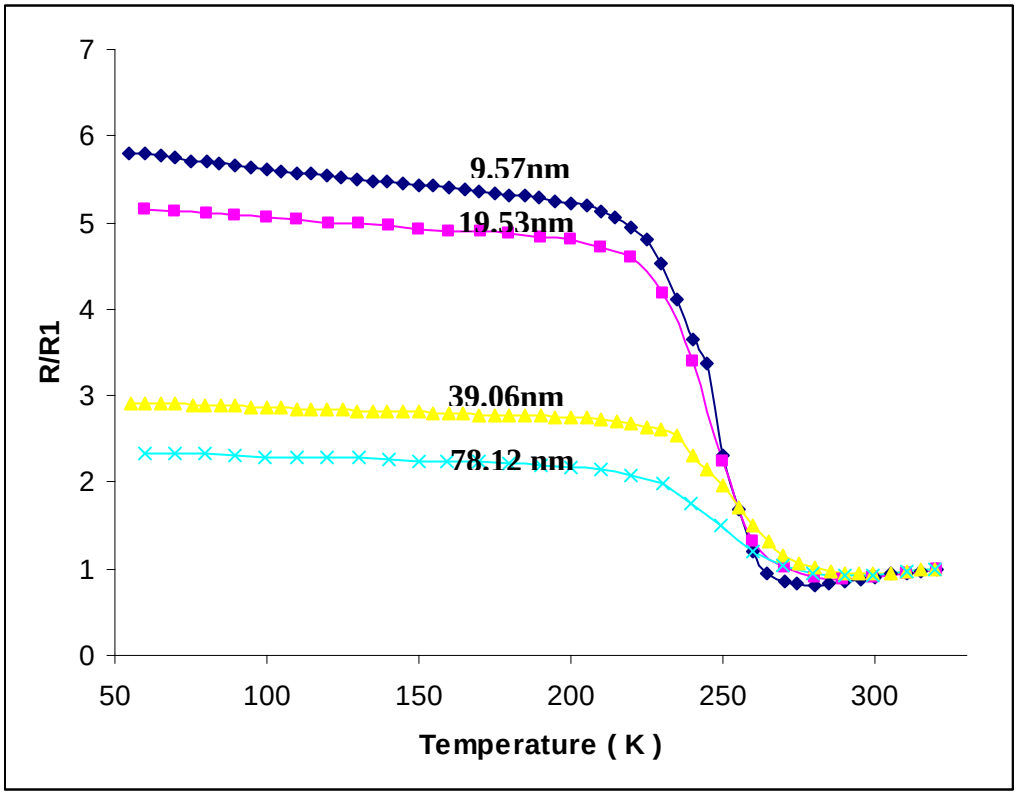

Figure 6.4.1 Thickness dependence on the transition FeSi films deposited at high fluence (3.5 J/cm^2).

Transitions observed for the films at different thicknesses, deposited at 3.5 J/cm^2 are shown in the figure 6.4.1. As can be seen in the figure, at high fluence, there is a distinguishable fall in the transition magnitude as more material is deposited on the substrate. It can rather be inferred that the reduction in the observed low temperature resistance could be due to the deeper diffusion of Fe ions into the substrate and lower resistance seen in thicker films could be due to the higher number of Fe^{++} ion diffusion with the increase in the deposition time. However it is profound that transition observed for the thinnest films was much lower than the originally observed four order of magnitude transition in the films deposited at very low fluence.

Summary

Experimental data discussed in the section 6.1 clearly indicates that the transition is effected by the laser fluence. The transition magnitude changed from 1MΩ for the FeSi films deposited at low fluence to 50Ω for the films deposited at high fluence. Furthermore, Ion probe study performed at different fluences showed an increase in the ion density and the kinetic energy of Fe ions in the ablated plasma with increase in laser fluence.

Chapter 7

Discussion and conclusions

All the silicon substrates used in this study contained a native SiO_2 layer of thickness 15-20nm. In a typical SiO_2 surface the defects give rise to a surface charge. For a very thin SiO_2 layer the charges tunnel to the SiO_2/Si interface to create interface state that causes the bands to bend. These effects forms Schottly barriers at the SiO_2/Si interface as shown in the figure 7.1.1. From the band diagrams it is clear that current transport through such junction formed is highly resistive due to the high band gap barrier of SiO_2. However, presence of impurities in SiO_2 forms an impurity band near the mid-band Fermi level that allow electrons to under go an impurity assisted tunneling process.

Even for room temperature growth Fe diffusion through the SiO_2 layer has been reported by K.Ruhrnschopf et al . [K.Ruhrnschopf et.al (1997)]. However due to the diffusion of Fe ions in to the interface, enhancement in the density of states in the SiO_2/Si interface can be expected give rise to an accumulation layer near the interface as shown in the Figure 7.1.2. Presence of an accumulation layer on a *p*-type substrate makes an Ohmic contact to the silicon substrate, therefore provides a low resistance path for current flow. Diffusion of iron into the SiO_2 layer in its multiple valance states Fe^0, Fe^+, Fe^{++} and Fe^{+++} will also form an impurity band within the large band gap of insulator. Observed low resistance at high temperatures can be considered to be due to the carrier hopping through the highly insulating SiO_2 layer as shown in the figure 7.1.2.

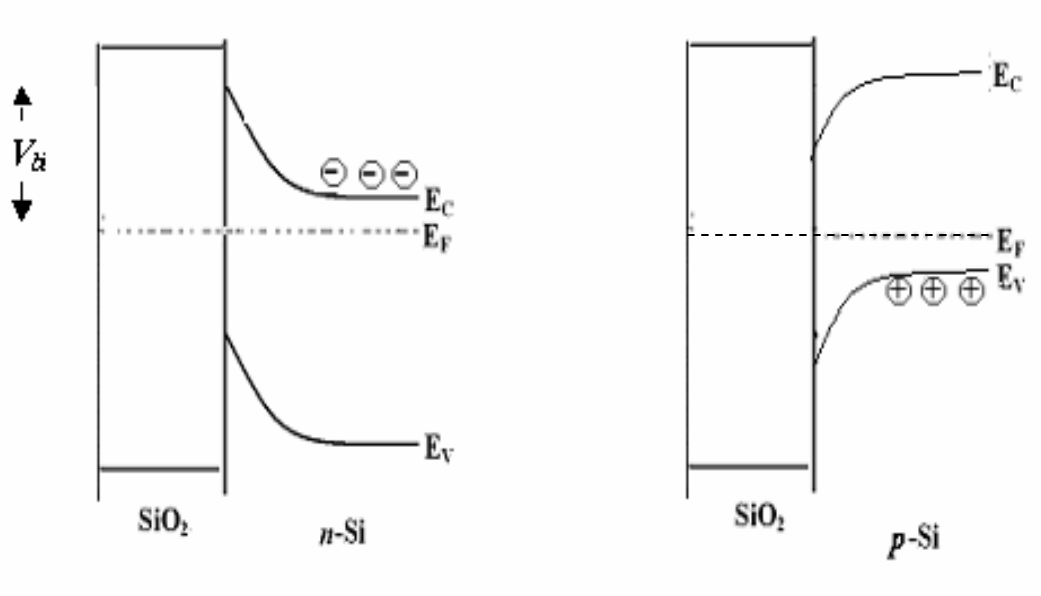

(a) (b)

Figure 7.1.1 Band bending SiO_2/Si interface for a) n- and b) p-type substrates.

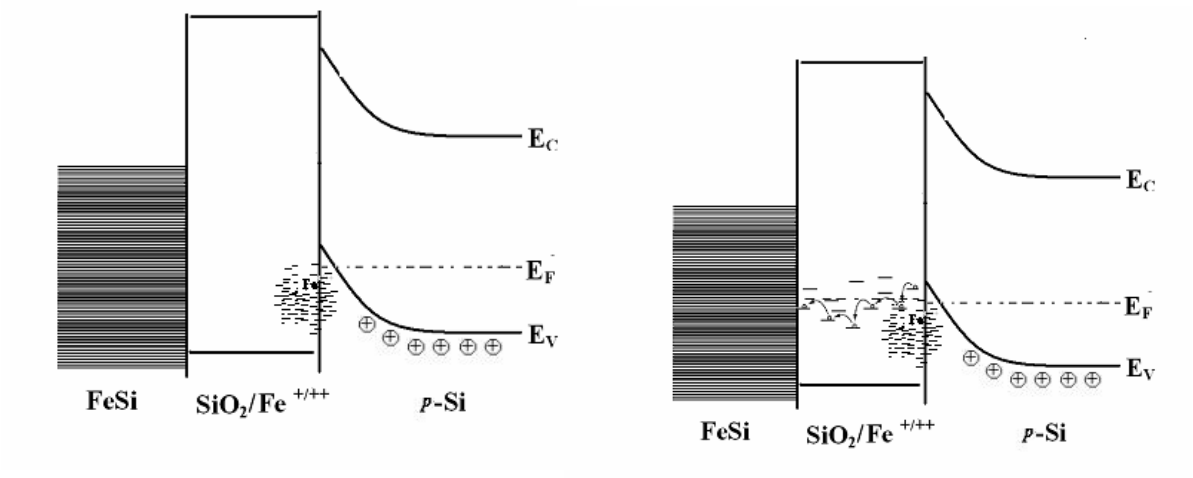

Figure 7.1.2 Accumulation and carrier hoping through the SiO_2 layer

The increase in resistance observed below the temperature of 250 K indicates the disruption of the accumulation condition. This can happen if a magnetic interaction between the Fe atoms (ions), such as an exchange interaction, causes the electrons to be localized at Fe sites. This would reduce the density of interface states that would change the accumulation layer into a depletion layer at the SiO2/Si interface. . Thus, below the transition temperature SiO_2/Si interface is assumed to change back to depletion situation (Figure 7.1.1) causing a rapid decrease in the hopping conduction through the oxide layer and as a result of this resistance starts to increase rapidly.

When potential is applied to the diode gate, the bands at the Si/SiO2 interface undergoes bending depending on the applied voltage polarity and magnitude. Considering the p-type silicon, a negative potential (V<0 or -I) applied to the attract mobiles holes in silicon towards the surface and an accumulation layer will be formed at the Si/SiO2 interface as shown in the Figure 7. 1.3c. The concentration of the holes in this layer will be higher than the hole concentration away from the surface in the silicon bulk and this situation is usually known as accumulation. Furthermore, when higher positive gate potential (V>0 or +I) is applied the holes at the surface will be repelled, but at the same time the electrons that are minority carriers in the p-type silicon will be attracted to the surface (Figure 7.1.3e), and as a result, the silicon surface will behave like an *n*-type rather than *p*-type. This situation usually called as inversion. Similarly, inversion and accumulation situations for the *n*-type silicon are shown in the Figures 7.1.3d and 7.1.3f.

Looking at the figures in Figure 7.1.3, the different resistance behaviors observed for isolated FeSi/SiO_2/Si systems for different directions of the currents in the section 5.1

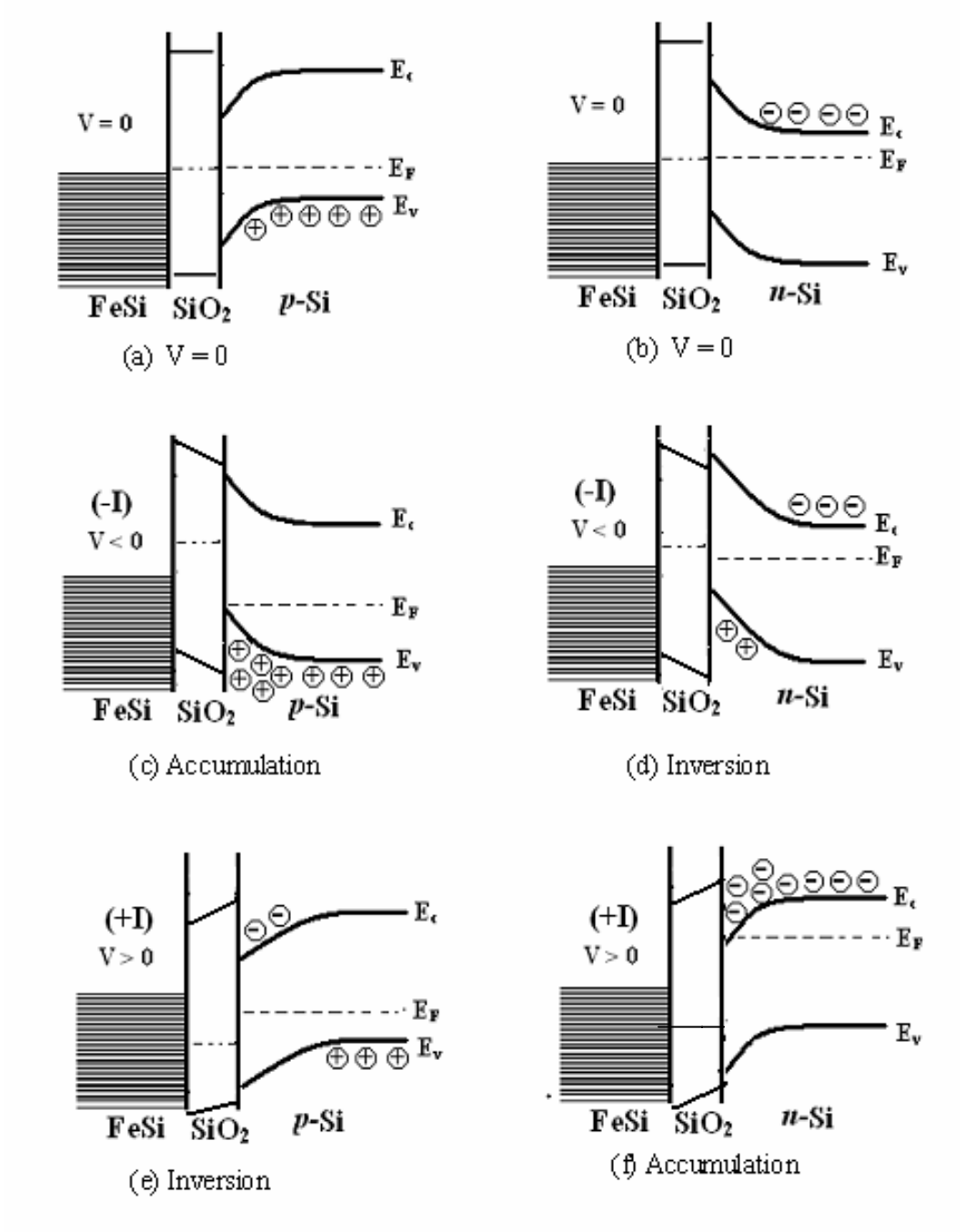

Figure 7.1.3 Energy band bending for various applied potentials for $FeSi/SiO_2/Si$ systems.

(Figures 5.1.7 and 5.1.8) can be attributed to the having more carrier concentration in accumulation than inversion situation for both *p*- and *n*-type silicon. Therefore it is clear that forward bias (V>0, +I) resistance is much higher than the reveres bias (V<0, -I) resistance for FeSi/SiO_2/*p*-Si systems, whereas oppositely for the FeSi/SiO_2/*n*-Si systems. Also, as current is increased, bias voltage is increased and this wills results more carrier accumulation in the interface resulting a lower resistance for higher current values. We observe similar current dependence in the resistance in the Figures 5.1.7 and 5.1.8. Accumulation and inversion situations observed in the band diagrams are also supported by the experimental data obtained in the Hall voltage experiments in the section 5.3.

IV data in the section 5.2 also indicated a Zener breakdown behavior in the reverse bias direction for isolated FeSi/SiO_2/*p*-Si and in the forward bias direction for the FeSi/SiO_2/*n*-Si systems. Due to the accumulation situations seen in Figures 7.1.3c and 7.1.3d, an electric filed is expected to build up between SiO2 layer, which gives sufficient energy for charges to tunnel through the insulating layer causing the observed Zener breakdown in the IV curves.

Furthermore, observed transition for the discontinuous FeSi films rules out the idea of current transport through the low resistive inversion layer formed at the surface of the silicon substrate as described by Dai et al [J.Dai et al (2000)]. Discontinuity of the film leads to a similar discontinuity of the inversion layer and thus such current transport through the inversion layer would be impossible.

Experiments performed on discontinuous metal coatings (Al and Pt) on bare Si substrates and metal coatings on FeSi grown films indicated that role of the presence of magnetic material to obtain the transition. However, after annealing the discontinuous Al

coatings we observed a formation of a perfect Ohmic contact with the silicon substrates due to the diffusion of Al through the SiO2 layer. This also conforms that Fe diffusion is expected in room temperature pulse laser deposited FeSi films.

Experimental data discussed in the section 6.1 clearly indicates that the transition is enormously effected by the laser fluence showing a dramatic change in the transition magnitude from 1MΩ for the FeSi films deposited low fluence into 50Ω for the films deposited at high fluence. Ion probe study also indicates an increase in the ion density and the kinetic energy of Fe ions in the ablated species with the increase of the laser fluence. Therefore, it can be inferred that, as the fluence is increased there is a deeper diffusion of Fe ions into the Si substrate due to the higher momentum of the species and higher concentration of Fe diffusion due to the higher ion concentration in the plume. As discussed in the beginning of this chapter, low resistive charge transport is formed in FeSi/SiO_2/Si systems through the impurity states located in the high band gap SiO_2 layer due Fe diffusion. Also due to the higher ion concentration of diffused ion near the SiO_2/Si interface an accumulation situation is expected even bellow the transition temperature.

Also under the equilibrium conditions the states at the SiO_2/Si interface cause the Fermi level to be pinned leading to a built-in potential of V_{bi}. For an abrupt junction with an impurity density of N the depletion layer width in p-silicon can be written in the form

$$\mathrm{W} = \sqrt{\frac{2\varepsilon}{qN}\left(V_{bi} - V - \frac{kT}{q}\right)}$$

where ε is the permittivity of the semiconductor, q is the electron charge, and T is the temperature. The impurity concentration near the interface is altered by the diffusion of

Fe into silicon and we can expect higher impurity concentration for the films deposited at higher fluences. Thus we can expect lower resistance as the depletion layer width is decreased with the increase of "*N*" .

Consequently, the hopping conductivity will vary as

$\sigma_{hop} \alpha \exp -[2\alpha R_D + W_D/kT]$,

where W_D is the activation energy for hopping through impurity states and R_D is the average distance between impurity states.

At the high fluence due to the higher impurity concentration, one can expect a rapid decrease in the average distance between impurity states (R_D) and thus a higher hopping conductivity. It can also be inferred that in the FeSi films deposited at higher fluence, charge transport through the substrate even bellow the transition temperature as the current path through the substrate is less resistive than that through the film. Thickness dependence on the transition observed in the FeSi films deposited at high fluence also expected due to the higher diffusion concentration with the increase in the deposition time.

In summary, this thesis presented a systematic set of experiments carried out on understanding the current transport in the metal-to-insulator transition observed in FeSi/SiO2/Si systems and the systematic set of experiments performed to understand the laser fluence dependence on the transition.

References

1) Bagwell P F, Park S L, Yen A, Antoniadis D A, Smith H I, Orlando T P and Kastner M A 1992 *Phys. Rev.* B **45** 9214

2) Chainani A., T. Yokoya, T. Morimoto, T. Takahashi, S. Yoshii, and M. Kasaya Phys. Rev. B 50, 8915–8917 (1994)

3) Dai J, L Spinu[1], K-Y Wang[1], L Malkinski[1] and J Tang[1,2] J. Phys. D: Appl. Phys. **33** No 11 (7 June 2000) L65-L67

4) Ferry D.K., ibid 2, 504 (1984)

5) Fuoss P. H. and L. J. Norton Phys. Rev. Lett. 60, 600–603 (1988)

6) Galkin N. G., D. L. Goroshko, S. T. Krivoshchpov, and E. S. Zakharova,

7) Jaccarino V, Wertheim G K, Wernick J H, Walker L R and Arajs S 1967 *Phys. Rev.* 160 476

8) Kaidanov V I, Tselishchev V A, lesalniek 1 K, Dudkin L D, Vomnov B K and Trusova N N 1968 *Sov.*

9) Krivanak O.L.,D.C. Tsui, T.T. Sheng, and A. Kamgar, The physics of SiO2 an its interface edited by Sokrates T. Pantelides

10) Lile D.L., J.Vac. Technol B4 496 (1984)

11) Liu Z., M. Okoshi, and M. Hanabusa, Rev. Laser Eng. **26**, 90 _1998_.

12) Lundstrom I., M.Amgarth, and L.G. Petersson CRC Crit.Rev.Solid State Mater.Sci 15,201 (1989)

13) Matthesis L.F. and D.R. Hamann, Physical Review B 47 13114 (1993)

14) McWhan D. B., T. M. Rice, and J. P. Remeika Phys. Rev. Lett. 23, 1384–1387 (1969)

15) Mossanek R.J.O. and M. Abbate* Caixa Postal 19091, 81531-990 Curitiba PR, Brazil

16) MOTT N. F. Rev. Mod. Phys. 40, 677–683 (1968)

17) Rajeswaran G., W.A.Anserson, M. Jackson, and M. Thayer, Thin Solid Films 104, 351 (1983)

18) Ruhrnschopf K., D.Borgman and G.Wedler, Surf.Sci. 374,269 (!997)

19) Ruthrnschopf K., D. Borgmann and G. Wedler, Thin Solid

20) Schlesinger Z.,Z.Fisk,H.T.Zhang,M.Bmaple, Physica B, 237-238,460,(1997).

21) Voˇcaldo L, Price G D and Wood I G 1999 Acta Crystallogr. B 55 484

22) Watanabe H., H. Yamamoto, and K. Ito, J. Phys. Soc. Jpn. 18, 995 (1963).

23) Watanak H. *Yamatnoto* H and *110* K 1963 *J. Phys.* Soc. *Japan* 18 991

24) Wertheim G.K., V. Jaccarino, J.H. Wernick, J.A. Seitchik, H.J. Williams, and R.C. Sherwood, Phys. Lett. 18, 89 (1965).

25) Wieder H. H. Journal of Vacuum Science and Technology Volume July (1978)

26) Witanachchi S., H. Abou Mourad, and P. Mukherjee J. Appl. Phys. 99, 073710 (2006)

27) Wolfe R, Wemick J H and Haszko S E 1965 *Phys. Le&* 19 449

Bibliography

1) Electrical Characterization of Semiconductor by P.Blood and J.W. Orton

2) Electronic Processes in Non-Crystaline Meterials

3) Metal-Insulator transitions by Sir Nevill Mott

4) Metal-Insulator Transitions revisited by P.P. Edwards, C.N.r.Rao

5) Physics Of Semiconductor Devices S.M Sze

6) Pulsed Laser Deposition of Thin films by Dougalas B Chrisey, Graham K.

7) Semiconductor Devices Physics and Technology by S,M Sze

8) Semiconductor Optoelectronic devices by Pallab Bhattacharya

9) Thyristor Physics by Adollph Blicher